



HAL
open science

3D structure enhancers based on functionalized MIL-53(Al) for improved dimethyl carbonate/methanol pervaporative separation

Katarzyna Knozowska, Joanna Kujawa, Tadeusz Muziol, Anthony Szymczyk, Wojciech Kujawski

► To cite this version:

Katarzyna Knozowska, Joanna Kujawa, Tadeusz Muziol, Anthony Szymczyk, Wojciech Kujawski. 3D structure enhancers based on functionalized MIL-53(Al) for improved dimethyl carbonate/methanol pervaporative separation. *Journal of Membrane Science*, 2024, 695, pp.122442. 10.1016/j.memsci.2024.122442 . hal-04431754

HAL Id: hal-04431754

<https://hal.science/hal-04431754v1>

Submitted on 16 May 2024

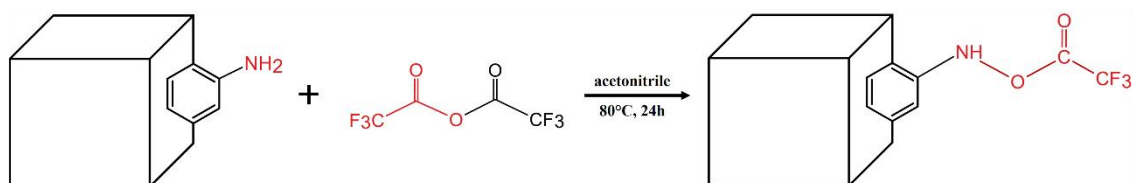
HAL is a multi-disciplinary open access archive for the deposit and dissemination of scientific research documents, whether they are published or not. The documents may come from teaching and research institutions in France or abroad, or from public or private research centers.

L'archive ouverte pluridisciplinaire **HAL**, est destinée au dépôt et à la diffusion de documents scientifiques de niveau recherche, publiés ou non, émanant des établissements d'enseignement et de recherche français ou étrangers, des laboratoires publics ou privés.

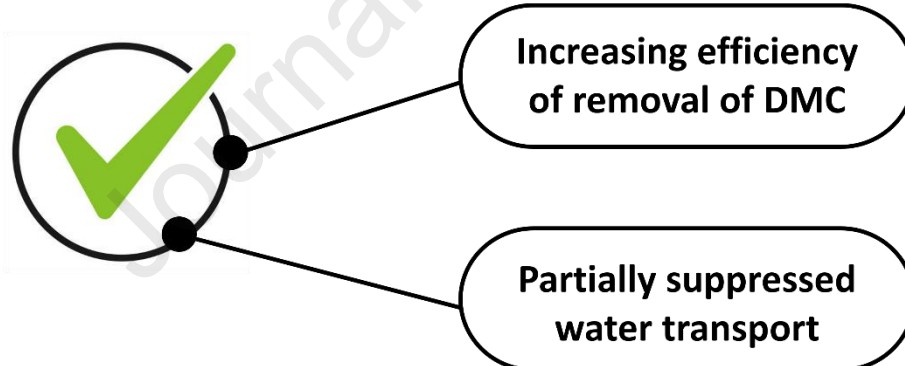
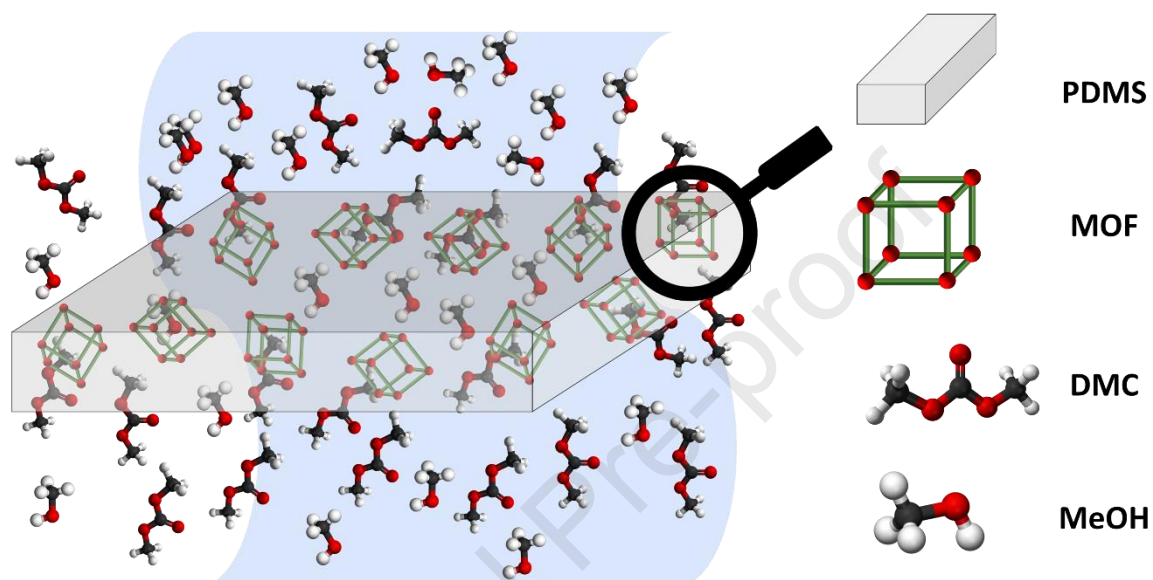


Distributed under a Creative Commons Attribution - NonCommercial 4.0 International License

Synthesis of hydrophobized analogue of MIL-53(Al)



Pervaporation of azeotrope mixture of DMC/MeOH (30 wt%:70 wt%)



1 **3D Structure Enhancers Based on Functionalized MIL-53(Al) for Improved**
2 **Dimethyl Carbonate/Methanol Pervaporative Separation**

3
4
5 Katarzyna Knozowska¹, Joanna Kujawa¹, Tadeusz Muzioł², Anthony Szymczyk³,
6 Wojciech Kujawski^{1,*}

7
8
9 ¹Membranes and Membrane Techniques Research Group, Faculty of Chemistry,
10 Nicolaus Copernicus University in Toruń, 7 Gagarina Street, 87-100 Toruń, Poland

11 ²Department of Inorganic and Coordination Chemistry, Faculty of Chemistry,
12 Nicolaus Copernicus University in Toruń, 7 Gagarina Street, 87-100 Toruń, Poland

13 ³Univ Rennes, CNRS, ISCR (Institut des Sciences Chimiques de Rennes) – UMR 6226,
14 F-35000 Rennes, France

15
16 *corresponding author: w.kujawski@umk.pl (WK)

17
18
19 **Abstract**

20 Dimethyl carbonate (DMC) is considered an alternative, green solvent. This paper focused
21 on enhancement in membrane performance in DMC removal by pervaporation (PV)
22 from azeotropic mixture of DMC/methanol as a consequence of the incorporation of nanofiller
23 into a PDMS matrix. Engineering a hydrophobized analogue of MIL-53(Al)
24 (NHOCOCF₃-MIL-53(Al)) as nanoenhancers for improved membrane materials is presented.
25 XRD analysis confirmed the successful synthesis of MOFs and proved that modification
26 does not influence crystalline structure of MOF, which is well retained. Properties
27 of the membranes in PV were assessed employing separation factor (β) and thickness-
28 normalized Pervaporation Separation Index (PSI_N). Modified PDMS membranes possess better
29 separation properties compared with pristine one. Results revealed that the incorporation of 5
30 wt% of NHOCOCF₃-MIL-53(Al) caused an increase of β from 3.1 to 3.7, a significant value
31 for organic-organic PV. Essential part of the work was to analyze impact of the presence
32 of water in the feed on overall membrane effectiveness. It was observed that in the case of traces
33 amount of water in the feed solution, water was preferentially transported from the feed
34 to the permeate side. However, the transport of water through membranes was partially
35 suppressed when water content in the feed was over 0.7 wt%.

36 1. Introduction

37 Dimethyl carbonate (DMC) is considered as an alternative, green solvent characterized
38 by low toxicity and good biodegradable properties [1]. DMC is being widely used in various
39 industries. In the petrochemical industry, DMC is added to petrol to enhance the octane number
40 [2]. DMC can also replace harsh solvents such as dimethyl sulfate and phosphate in the reaction
41 of methylation and carbonylation [3].

42 There are several routes of synthesis of dimethyl carbonate, however, the most common
43 are phosgenation of methanol and oxy-carbonylation of methanol or methyl nitrile process [1].
44 During the synthesis of DMC, an excess of methanol is used, therefore resultant mixture
45 consists of dimethyl carbonate and unreacted methanol. The post-reaction mixture cannot
46 be separated easily by distillation as dimethyl carbonate and methanol create the azeotrope
47 mixture, containing 70 wt% of methanol [4]. Several methods have been proposed
48 for the separation of an azeotropic mixture of dimethyl carbonate/methanol such as pressure
49 swing distillation, extractive distillation, and membrane separation techniques. Comparing all
50 available methods, membrane separation techniques, especially pervaporation, appears
51 to be a good alternative to the classical separation methods [5]. Moreover, owing
52 to the different mechanisms of separation, pervaporation overcomes the vapour-liquid
53 equilibrium of azeotropic mixtures [6].

54 Several types of membranes have been evaluated for the separation of DMC/methanol
55 mixture by pervaporation methanol selective membranes (such as chitosan – CS [6], poly(vinyl
56 alcohol) – PVA [7], poly(acrylic acid) – PAA [8]) and dimethyl carbonate selective membranes
57 (such as poly(dimethylsiloxane) – PDMS [9] or poly(vinylidene fluoride) – PVDF [10]).
58 However, it should be mentioned that methanol is a major component of the azeotropic mixture
59 (70 wt%). The application of methanol selective membranes would require much more energy
60 used for the separation compared to the use of DMC selective ones. Therefore, it could be more
61 reasonable to apply hydrophobic membranes for the separation of dimethyl carbonate/methanol
62 mixtures owing to the affinity between the membrane material and the separated mixture.

63 Moreover, it should be mentioned that binary mixtures of organic solvents always
64 contain traces of water (the third component). The presence of water in a separated mixture
65 is an important factor influencing and limiting the overall efficiency of organic-organic
66 pervaporation. In our previous research [11, 12] we tested both hydrophobic (PDMS)
67 and hydrophilic (PVA) polymeric membranes in the separation of an ethyl *tert*-butyl
68 ether/ethanol (ETBE/EtOH) mixture. Research showed that the PDMS membrane selectively

69 transported ETBE while for the PVA membrane, EtOH was selectively transported.
70 Additionally, during experiments, the transport of water through the membranes
71 was also investigated. The comparison of water transport for the PDMS and PVA
72 was performed for mixture of ETBE/EtOH containing an equal amount of ETBE/EtOH mixture
73 and ca. 0.30 wt% of water. It was found that water was present also in the permeate.
74 However, a lower amount of water in permeate was noticed for the PDMS membrane.
75 In this case, the water content in permeate was equal to 0.14 wt%, while during the experiment
76 with the PVA based membrane, 3.21 wt% of water was detected. During the pervaporation
77 process, the membrane swells, which results in the free volume increase and this facilitates
78 the transport of separated components. Water is characterized by a smaller kinetic diameter
79 (2.65 \AA [13]) compared with organic solvents ($\geq 3.6 \text{ \AA}$ [14]). Therefore small water molecules
80 can easily pass through both hydrophilic and hydrophobic membranes. However, taking
81 into account the hydrophobic character of PDMS membranes, the transport of water during
82 the separation of organic solvent mixtures is reduced. Based on these results,
83 it can be concluded that hydrophobic membranes would be a better choice for the separation
84 of polar/nonpolar organic mixtures if the nonpolar component should be removed.

85 Among various hydrophobic polymers, PDMS appears as a good material
86 for the membrane preparation for the removal of DMC from DMC/methanol mixture
87 [9, 10, 15, 16]. PDMS is characterized by good film-forming properties, low cost, and excellent
88 mechanical and chemical stability [17]. However, polymeric membranes show
89 permeability/selectivity trade-off limitations [18-21]. To overcome that issue, various fillers
90 can be incorporated into the polymer matrix to prepare Mixed Matrix Membranes (MMMs).
91 Owing to the good compatibility with the polymer matrix, tunable structure, and possibility
92 of functionalization, metal organic frameworks (MOFs) have been extensively used as fillers
93 for the preparation of MMMs [22].

94 MIL-53(Al) (Materials Institute Lavoisier-53) is an excellent candidate
95 for a filler for the preparation of pervaporative MMMs. MIL-53(Al) consists of corner-sharing
96 $\text{AlO}_4(\text{OH}_2)$ octahedral coordinated by benzene-1,4-dicarboxylate linkers (BDC) [23].
97 This MOF is characterized by very good thermal and chemical properties and stability in water
98 [24, 25]. Qian et al. [26] investigated the stability of MIL-53(Al) in an aqueous solution
99 at pH equal to 2, 7, and 14. Results showed that MIL-53(Al) demonstrated excellent resistance
100 to hydrolysis at pH=2 and pH=7. After 7 days of soaking in acidic or neutral aqueous solution
101 at a temperature equal to 50°C and 100°C , practically no changes in crystalline structure
102 were observed. Only at pH=14, MIL-53 particles show limited stability, i.e., after 2 days

103 of soaking in a basic aqueous solution the gradual degradation of the crystalline structure
104 was noticed [26].

105 MIL-53(Al) belongs also to the special group of MOFs called “*breathing*” MOFs
106 [27-29]. MIL-53(Al) possesses the ability to change the framework conformations from narrow
107 pores “*np*” to large pores “*lp*” in the presence of guest molecules trapped inside the pores.
108 The *breathing* effect depends on the amount and the nature of guest molecules
109 and in the case of MIL-53, this effect is reversible [29]. Mounfield and Walton [30]
110 investigated the influence of solvothermal preparation methods on the *breathing* properties
111 of MIL-53(Al). It was noticed that MIL-53(Al) synthesized with N,N-dimethylformamide
112 (DMF) at 120°C did not demonstrate the *breathing* effect, whereas the MIL-53(Al) synthesized
113 with DMF at 220°C showed a slight, gradual *breathing* effect [30].

114 Several studies indicated that MIL-53(Al) might absorb water from the atmosphere
115 [24, 31, 32]. This property may limit the usage of MIL-53(Al) in processes where water
116 is an undesirable component. Therefore, the best solution is to additionally hydrophobize
117 MIL-53(Al). There are two ways to hydrophobize MIL-53(Al), i.e. during the synthesis
118 (application of ionic liquid as solvent [31]) or during the post-synthesis modification
119 (incorporation of modulators possessing a hydrophobic alkyl chain [33]).

120 In this work, hydrophobic and heterogeneous PDMS based membranes
121 with MIL-53(Al) and its analogues, i.e., NH₂-MIL-53(Al) and NHOCOCF₃-MIL-53(Al)
122 were fabricated for the selective removal of dimethyl carbonate from azeotropic dimethyl
123 carbonate/methanol mixture. Hydrophobic NHOCOCF₃-MIL-53(Al) was obtained during
124 the post-synthesis modification of NH₂-MIL-53(Al) with a hydrophobic modulator
125 i.e., trifluoroacetic anhydride. Modification of NH₂-MIL-53(Al) adjusted the interaction
126 between the MMM and the separated mixture resulting in an increase in MMMs performance.
127 Moreover, the influence of the presence of water in the separated mixture on the efficiency
128 of organic-organic pervaporation was also investigated and evaluated.

129

130 2. Experimental

131 2.1 Materials

132 Silicone rubber compounds (RTV615A and RTV615B) were delivered by Momentive
133 Performance Materials (Waterford, USA).

134 Aluminium nitrate nonahydrate ($\text{Al}(\text{NO}_3)_3 \cdot 9\text{H}_2\text{O}$), acetonitrile anhydrous (99.8%),
135 and dimethyl carbonate *ReagentPlus*® (99%) (DMC) were purchased from MilliporeSigma
136 (Milwaukee, USA). Benzene-1,4-dicarboxylic acid (BDC)
137 and 2-aminobenzene-1,4-dicarboxylic acid (NH_2 -BDC) were provided by Acros Organic
138 B.V.B.A. (Geel, Belgium). Trifluoroacetic acid anhydrous (TFA) was acquired from abcr
139 GmbH (Karlsruhe, Germany). Methanol, ethanol, acetone, N,N-dimethylformamide (DMF),
140 and hexane were supplied by Chempur (Piekary Śląskie, Poland). All solvents were utilized
141 as received without further purification. 15 M Ω cm reverse osmosis water (Hydrolab sp. z o.o.,
142 Straszyn, Poland) was used.

143

144 2.2 Synthesis of MIL-53(Al)

145 MIL-53(Al) was synthesized according to the procedure proposed by Mounfield and
146 Walton [30] with some modifications. In brief, 2.246 g of $\text{Al}(\text{NO}_3)_3 \cdot 9\text{H}_2\text{O}$ and 0.895 g of BDC
147 were dissolved in 30 mL of DMF in a Schott glass bottle at room temperature.
148 Subsequently, the obtained solution was placed in an oven and heated at 120°C for 12h.
149 After a slow cooling down, the whitish solution was centrifuged (4500 rpm, 30 min)
150 and washed 3 times in DMF and 3 times in acetone. In the final step, MIL-53(Al)
151 was dried at 100°C for 12 h.

152

153 2.3 Synthesis of NH_2 -MIL-53(Al)

154 NH_2 -MIL-53(Al) was synthesized as described in [34]. 0.76 g of $\text{Al}(\text{NO}_3)_3 \cdot 9\text{H}_2\text{O}$
155 and 0.56 g of BDC- NH_2 were dissolved in 15 mL of water and DMF, respectively.
156 Subsequently, the solutions were mixed and placed in the oven at 150°C for 24h.
157 In the next step, a cooled yellowish solution of NH_2 -MIL-53(Al) was centrifuged (4500 rpm,
158 30 min) and activated by heating under reflux in DMF at 153°C for 5h. NH_2 -MIL-53(Al)
159 powder was washed 4 times in acetone, followed by a centrifugation (4500 rpm, 30 min).
160 In the final step, the product was dried at 30°C for 12h.

161

2.4 Modification of NH₂-MIL-53(Al) by trifluoroacetic anhydride

Prior to the modification, 1.5 g of NH₂-MIL-53(Al) was placed in the round bottom flask and heated at 150°C for 6 h. After cooling down, NH₂-MIL-53(Al) powder was suspended in 125 mL of acetonitrile, and 64 mL of trifluoroacetic anhydride was added to the suspension for incorporation of trifluoroacetic anhydride into the structure of NH₂-MIL-53(Al). Subsequently, the suspension was heated under the reflux at 80°C for 24h. The final product (NHOCOCF₃-MIL-53(Al)) was centrifuged and washed 4 times in chloroform. Finally, NHOCOCF₃-MIL-53(Al) was dried in an oven at 50°C for 12h [33]. The scheme of the modification is presented in Figure 1.

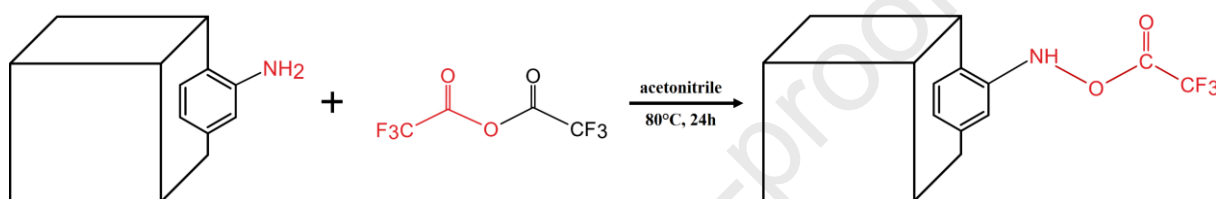


Figure 1. Scheme of the post-modification of NH₂-MIL-53(Al) by trifluoroacetic anhydride.

2.5 Preparation of pristine PDMS membrane

PDMS membranes were prepared using the phase inversion techniques induced by solvent evaporation. Components, i.e., RTV615A and RTV615B were dissolved in hexane. The obtained solution contains 15 wt% of polymer and the ratio of silicon crosslinker (RTV615B) with platinum catalyst to vinylfunctionalized prepolymer (RTV615A) was constant and equal to 1:10. In the next step, the obtained solution of PDMS was poured into a Teflon mould and left for the solvent evaporation. Finally, the membrane was crosslinked in an oven at 80°C for 2h.

2.6 Preparation of PDMS-based MMMs

PDMS-based MMMs were also prepared by the phase inversion technique -induced by solvent evaporation. A given amount of MIL-53(Al), NH₂-MIL-53(Al) or NHOCOCF₃-MIL-53(Al) was suspended in the previously prepared 15 wt% solutions of PDMS in hexane to fabricate the membranes containing 5, 10, or 15 wt% of fillers with regard to mass of the polymer. Subsequently, the PDMS solutions with fillers were mixed at room temperature for 24h and sonicated for 15 min. Casting and crosslinking of MMMs were done following the same procedure as used for the preparation of the pristine PDMS membrane samples.

2.7 Characterization of fillers and PDMS based membranes

XRD analysis of the crystalline structure of MIL-53(Al), NH₂-MIL-53(Al), and NHCOCF₃-MIL-53(Al) was performed using Philips X'Pert (Malvern Panalytical, Malvern, UK) in transmission mode with an X'Celerator Scientific detector with Cu anode. Scans were recorded in the range of 5-60° 2 θ . X'Pert Plus software (v. 1.0, Malvern Panalytical, Malvern, UK) was used for the data acquisition and processing.

FTIR-ATR spectra of MOF particles were accomplished using a Vertex 70V spectrometer (Bruker, Billerica, USA) in the range of 400-4000 cm⁻¹ with a resolution of 4 cm⁻¹ and a number of scans equal to 512. Results were analysed using OPUS software (v. 7.5, Bruker, Billerica, USA).

Particle size distribution of synthesized MOFs was analysed by dynamic light scattering (DLS) using LitesizerTM500 (Anton Paar, Graz, Austria) according to the procedure described elsewhere [35]. KalliopeTM software (v2.10.5, Anton Paar, Graz, Austria) was used for data analysis.

MOF particles were also analysed using high-resolution transmission electron microscopy (HR-TEM) with a Tecnai G2 F20 X-Twin microscope (200 kV, FEI Europe, B.V., Eindhoven, the Netherlands). Analysis was performed on a copper mesh and particles were suspended in ethanol.

The low-temperature nitrogen adsorption/desorption measurements of MIL-53(Al), NH₂-MIL-53(Al), and NHCOCF₃-MIL-53(Al) were accomplished using a Gemini VI instrument (Micromeritics Instrument Corp., Norcross, USA). Samples were first degassed at 110°C for at least 4h and then measurements were performed at around -200°C. The Brunauer-Emmett-Teller and the Barrett-Joyner-Halenda models were implemented for the calculation of specific surface area and pore volume, respectively.

Surface topography measurements of MOF particles and membranes were performed with a LEO 1430 VP microscope (Leo Electron Microscopy Ltd., Cambridge, UK). Prior to the analysis, a conductive layer of Au/Pd was sputtered on the surface of the samples.

NanoScope MultiMode SPM system (Veeco Digital Instrument Plainview, USA) was implemented in AFM analysis. Analysis was performed in a tapping mode with a nitride probe. Nanoscope software (v6.13, Bruker Optik GmbH, Ettlingen, Germany) was used for data analysis. The roughness parameter R_A was an average of 4 measurements with the scanned area equal to 5 $\mu\text{m} \times 5 \mu\text{m}$.

224 The thermal stability of synthesized MOF particles and fabricated membranes
 225 was tested using a TGA-DTA Thermal Analysis Instruments type SDT 2960 (TA Instrument,
 226 Champaign, USA). Tests were achieved at the temperature range of 25-1000°C
 227 under the nitrogen atmosphere. The heating rate during all measurements was equal
 228 to 10°C/min. TA Universal Analysis software (v5.5.24, TA Instrument, Champaign, USA)
 229 was implemented during the acquisition and processing of the results.

230 The apparent contact angles for water and diiodomethane were measured using
 231 a goniometer Attention Theta (Biolin Scientific, Gothenburg, Sweden). Experiments
 232 were conducted at room temperature. The drop volume of water and diiodomethane was equal
 233 to 2 µl. OneAttention software (v2.8 r 5543, Biolin Scientific, Gothenburg, Sweden)
 234 was used for the data acquisition and processing.

235 A thickness gauge Sylvac type S 299 was used for measuring the thickness of fabricated
 236 membranes. The resolution and accuracy of the measurements were equal to 0.001 mm
 237 and 0.002 mm, respectively.

238

239 2.8 Pervaporation experiments

240 All pervaporation measurements were conducted using a standard laboratory set-up
 241 equipped with a membrane module with an active membrane area equal to 14.5 cm² [36].
 242 Experiments were performed at 40°C ± 1°C. Dimethyl carbonate/methanol (DMC/MeOH)
 243 mixtures at the following mass ratios were used as feeds during pervaporation: 20/80, 30/70,
 244 50/50, 70/80, and 80/20

245 Performance (transport and separation properties) of the fabricated membranes
 246 were assessed using the thickness normalized total permeate flux ($J_{N,t}$), thickness normalized
 247 partial permeate flux ($J_{N,i}$), separation factor (β), and thickness normalized Pervaporation
 248 Separation Index (PSI_N) [37, 38].

249 Thickness normalized total permeate flux was calculated based on Eq. (1) [37]:

$$250 J_{N,t} = \frac{\Delta m}{A \cdot \Delta t} * l \quad (1)$$

251 where Δm is the mass of collected permeate [g], A active area of the membrane [m²],
 252 Δt time of collecting the permeate sample [h].

253 Thickness normalized partial permeate flux was estimated using Eq. (2)

$$254 J_{N,i} = J_{N,t} * y_i \quad (2)$$

255 where y_i is a mass fraction of component i in permeate.

256

257 Eq. (3) [37] was implemented to calculate the separation factor (β):

$$258 \quad \beta = \frac{y_i/(1-y_i)}{x_i/(1-x_i)} \quad (3)$$

259 where y_i is the mass fraction of component i permeate and x_i is the mass fraction of component
260 i in the feed.

261 Thickness normalised Pervaporation Separation Index (Eq. (4)) was applied
262 for the comparison of performances of various PDMS based membranes during the separation
263 of DMC/MeOH mixtures [38]. According to the definition, the higher the value
264 of this parameter, the more efficient membrane is in particle separation [39].

$$265 \quad PSI_N = l \cdot J_{N,t} \cdot (\beta - 1) \quad (4)$$

266 The influence of water presence in organic solvents on the overall efficiency
267 of pervaporation was also investigated using the enrichment factor of water (Eq. (7))
268 as a metric.

$$269 \quad EF_{water} = \frac{P_W}{F_W} \quad (7)$$

270 where P_W and F_W are the content of water in permeate and feed, respectively.

271

272 **2.9 Gas chromatography**

273 Shimadzu Nexis GC-2030 gas chromatograph (Shimadzu Corp., Kyoto, Japan)
274 with a TCD detector and Q Bond column was used to determine the feed and permeate
275 composition. The temperature of the column was programmed from 140°C to 180°C.
276 The set temperature of the TCD detector and injector was equal to 250°C and 220°C,
277 respectively. Obtained chromatograms were processed with Lab Solutions software
278 (v.5.106, Shimadzu Corp., Kyoto, Japan).

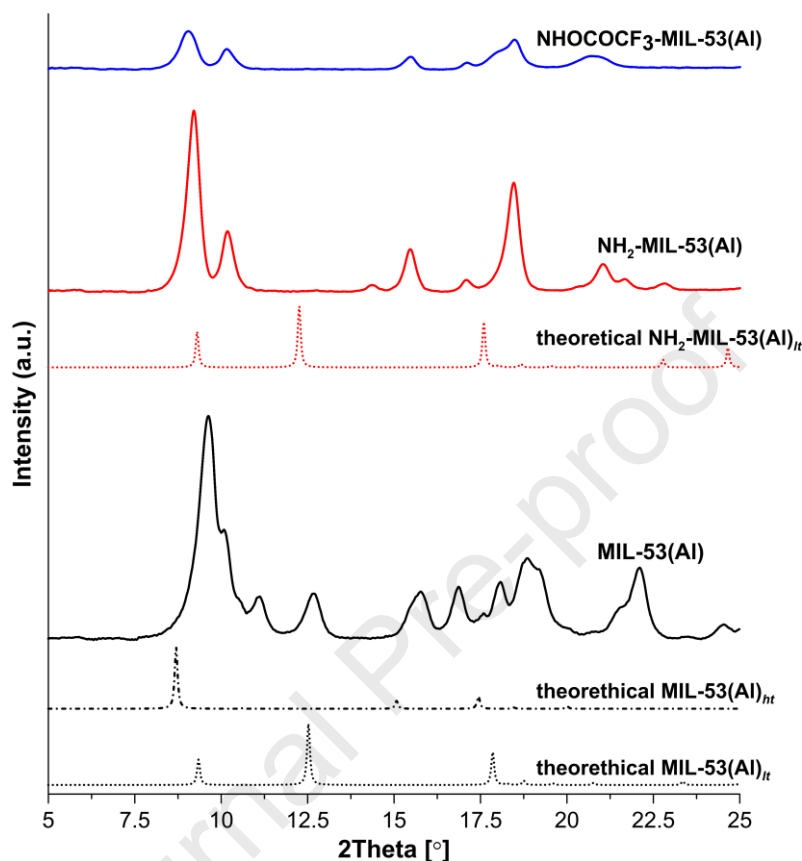
279

280 **3. Results and discussion**

281 **3.1 Characterization of MOF particles**

282 Synthesized MIL-53(Al), NH₂-MIL-53(Al), and NHOCOCF₃-MIL-53(Al)
283 were characterized using various analytical techniques. XRD patterns of synthesized MOFs
284 are presented in Figure 2. Based on these results, it can be concluded that MIL-53(Al)
285 and NH₂-MIL-53(Al) possess high crystalline structures. Synthesized MOF particles
286 can form an lp and np crystalline form structures with peaks at around 8.6° related to the lp
287 form crystallizing in the orthorhombic Imma space group, while the peaks at around
288 9.2 and 12.3° correspond to the np form crystallizing in the monoclinic Cc space group [24].

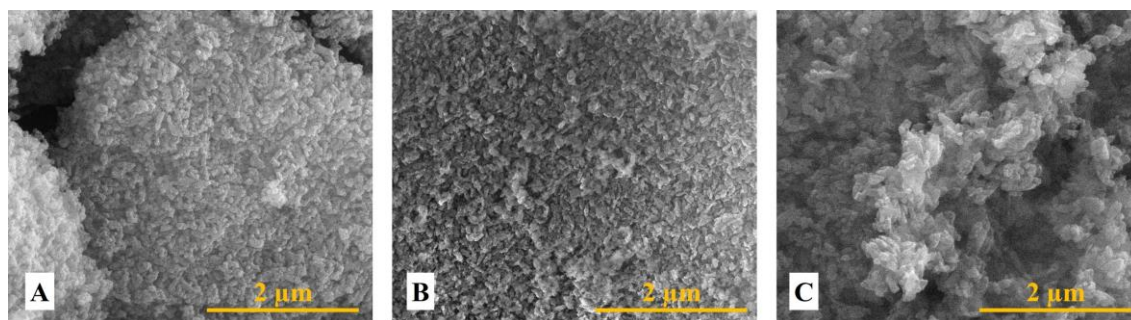
289 In the case of MIL-53(Al), characteristic peaks at 9.4 (200) and 12.4° (110) correspond
 290 to the low temperature (*lt*) phase while the peak at 10.8° (010) can be ascribed to high
 291 temperature (*ht*) structure.



292
 293 Figure 2. XRD pattern of MIL-53(Al), NH₂-MIL-53(Al), and NHOCOCF₃-MIL-53(Al).
 294

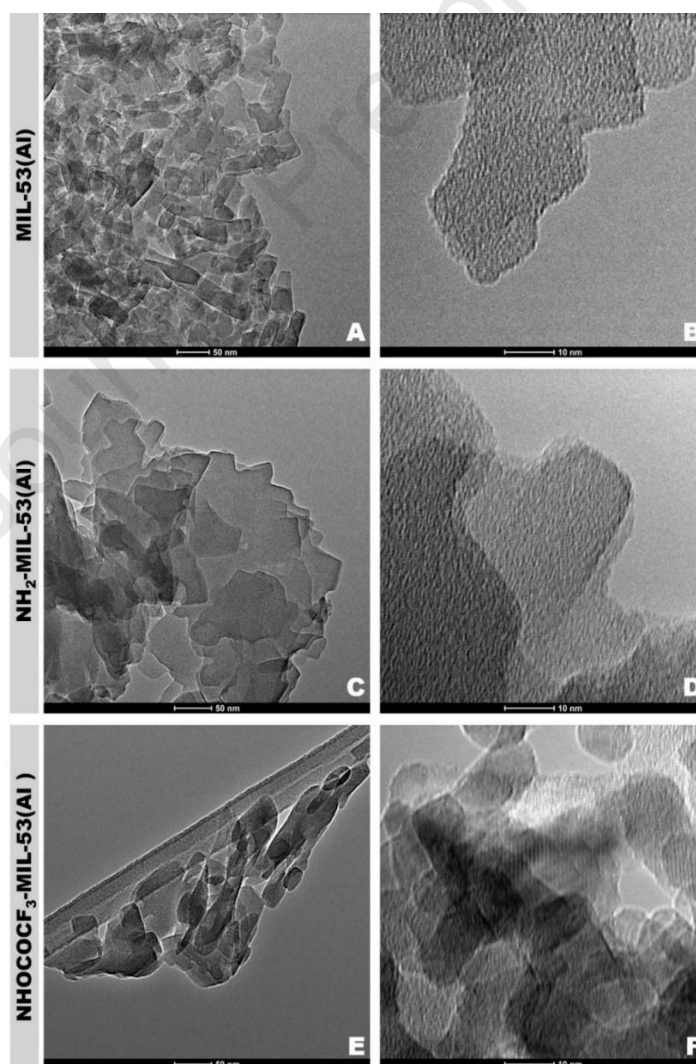
295 The XRD spectra of NH₂-MIL-53(Al) showed characteristic peaks of low-temperature
 296 structure (9.2° (200), 10.2° (200), and 18.4° (400) [40]) (Figure 2).
 297 As can be seen from Figure 2, the peaks are narrow and their positions indicate that mainly
 298 *np* form was obtained. Additionally, no peak at 8.6° related to the high-temperature structure
 299 was noticed. For NHOCOCF₃-MIL-53(Al) any single crystal model is not known.
 300 Nevertheless, it was noticed that after the modification, the peak positions were not altered
 301 and the crystalline structure of NH₂-MIL-53(Al) was retained (Figure 2). This indicated
 302 that the attachment of trifluoroacetic anhydride to NH₂-MIL-53(Al) does not change
 303 the crystalline structure of particles. These results are consistent with the work reported
 304 by Wu et al. [7].

305 The size and crystal morphology of synthesized MIL-53(Al), NH₂-MIL-53(Al),
 306 and NHOCOCF₃-MIL-53(Al) were investigated with Scanning (SEM) and Transmission
 307 (TEM) Electron Microscopy as well as Dynamic Light Scattering (DLS).



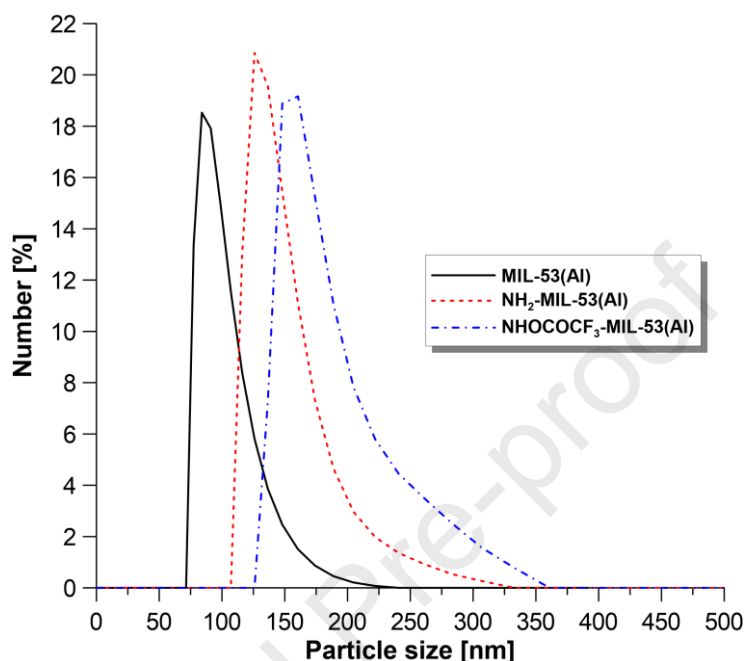
308
309 Figure 3. SEM micrographs of MIL-53(Al) – A, NH₂-MIL-53(Al) – B,
310 and NHOCOCF₃-MIL-53(Al) – C.

311
312 SEM pictures of obtained MOFs are presented in Figure 3. It was observed
313 that the MIL-53(Al) and NH₂-MIL-53(Al) crystallites showed a needle-like structure
314 (Figure 3A and B). In the case of NHOCOCF₃-MIL-53(Al) (Figure 3C), no significant change
315 in structure was noticed compared with the structure of the unmodified NH₂-MIL-53(Al).



316
317 Figure 4. TEM images of the synthesized enhancers. A and B – MIL-53(Al);
318 C and D – NH₂-MIL-53(Al); E and F – NHOCOCF₃-MIL-53(Al).

319 The crystallines were also analyzed by applying the TEM technique (Figure 4).
 320 From the images, it was possible to measure the size of the particles that were equal
 321 to 95 ± 15 nm for MIL-53(Al), 113 ± 28 nm for NH₂-MIL-53(Al), and 160 ± 28 nm
 322 for NHOCOCF₃-MIL-53(Al), respectively.

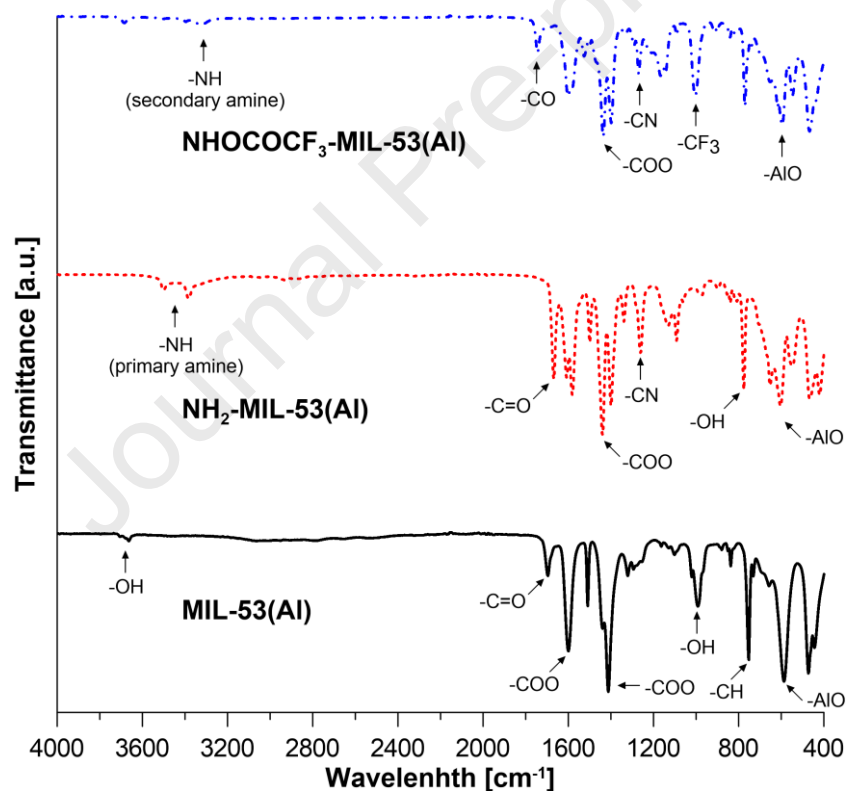


323
 324 Figure 5. Results of DLS analysis of MIL-53(Al), NH₂-MIL-53(Al), and NHOCOCF₃-MIL-53(Al).
 325

326 Synthesized MIL-53(Al), NH₂-MIL-53(Al), and NHOCOCF₃-MIL-53(Al) molecules
 327 were characterized by particle sizes in the range of 110 ± 10 nm, 125 ± 26 nm,
 328 and 160 ± 30 nm, respectively (Figure 5). A similar value of NH₂-MIL-53(Al) particle size
 329 was found by Nguyen et al. [34]. It should be mentioned that the size of MOF particles depends
 330 on the conditions of synthesis. Nguyen et al. [34] investigated the influence of solvents
 331 (DMF, water, and a mixture of water and DMF) used during the synthesis on the particle
 332 size of NH₂-MIL-53(Al). It was reported that the presence of water influences not only particle
 333 size but also the shape of obtained crystals. SEM analysis of NH₂-MIL-53(Al) demonstrated
 334 that when the water content in the mixture increased from 50 vol% to 70 vol%, the particle size
 335 increased from 127 nm to 419 nm [34].

336 FTIR-ATR analysis was performed to prove the successful modification of MIL-53(Al).
 337 Obtained FTIR-ATR spectra are presented in Figure 6. Analysing the obtained results,
 338 it can be stated that in all cases, the characteristic peaks of MIL-53(Al) were detected.
 339 Bands in the range of $3660\text{-}3707$ cm⁻¹ and 902 cm⁻¹ correspond to the vibration of OH groups
 340 from the aluminium cluster, while the peak at 587 cm⁻¹ is associated with AlO vibration

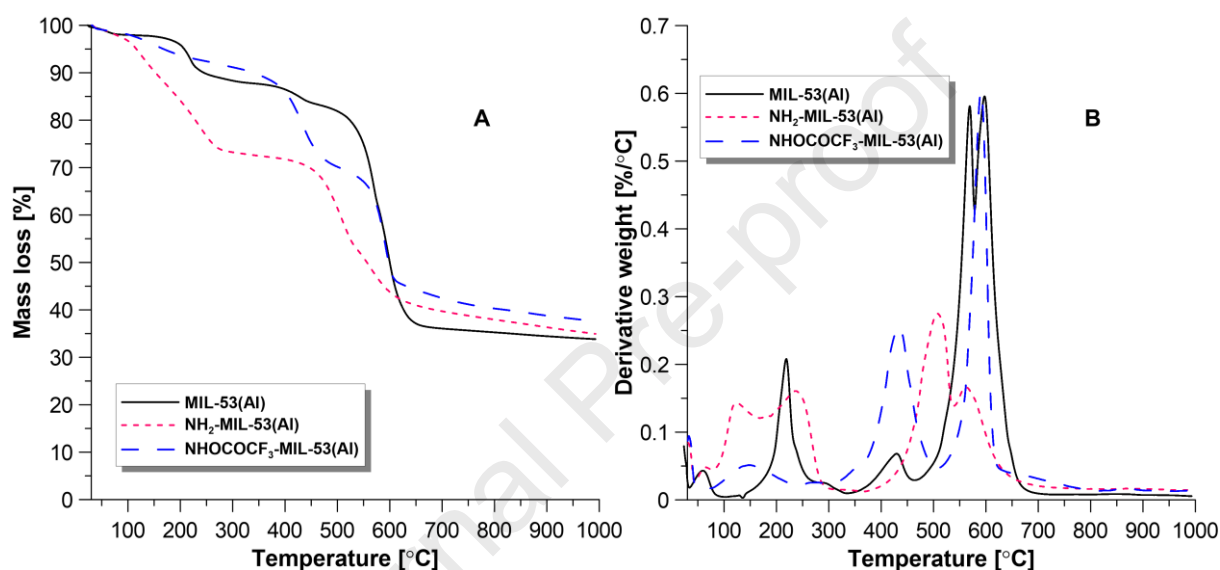
341 (Figure 6). The bands at 1602 cm^{-1} and 1412 cm^{-1} are related to the asymmetric stretching
 342 of the COO^- a group of BDC ligands. Bands at 1696 cm^{-1} and 753 cm^{-1} correspond
 343 to the vibration of C=O groups from the BDC ligands and the $-\text{CH}$ group, respectively.
 344 In the case of $\text{NH}_2\text{-MIL-53(Al)}$, additional bands have been detected. Bands in the range
 345 of $3385\text{ cm}^{-1} - 3503\text{ cm}^{-1}$ correspond to vibration from the amine group of $\text{NH}_2\text{-BDC}$ ligands
 346 (Figure 6). In the case of the modified $\text{NH}_2\text{-MIL-53(Al)}$ by the trifluoroacetic anhydride, peaks
 347 from $\text{NH}_2\text{-MIL-53(Al)}$ and trifluoroacetic anhydride were detected. It was found that after
 348 modification, bands from the primary amine disappeared and a new band from the secondary
 349 amine was observed (3325 cm^{-1}). Moreover, the additional peak from the symmetric stretching
 350 vibration of CF_3 groups (1005 cm^{-1}) was also found (Figure 6). Based on the obtained results,
 351 it can be concluded that the modification of $\text{NH}_2\text{-MIL-53(Al)}$ led to the successful
 352 incorporation of trifluoroacetic anhydride.



353
 354 Figure 6. FTIR spectra of synthesized MIL-53(Al), $\text{NH}_2\text{-MIL-53(Al)}$, and $\text{NHOCOCF}_3\text{-MIL-53(Al)}$.
 355

356 Thermogravimetric analysis of MIL-53(Al), $\text{NH}_2\text{-MIL-53(Al)}$,
 357 and $\text{NHOCOCF}_3\text{-MIL-53(Al)}$ is presented in Figure 7A and B. As it can be seen,
 358 the degradation of synthesized MOFs occurs through multiple stages. The mass loss
 359 of up to 300°C is related to the removal of guest molecules (DMF , H_2O). Next, mass loss
 360 in the temperature range of 300°C - 500°C corresponds to the condensation of the carboxylic

361 group and acid anhydrides are formed as a result of condensation [41]. Subsequently, starting
 362 from the temperature of 500°C-550°C, BDC, NH₂-BDC, and NHOCOCF₃-BTC ligands
 363 were detached from the structure and the collapsing of frameworks occurred (Figure 7A and B).
 364 Moreover, based on TGA the results, it can be indicated that the final product of thermal
 365 degradation of MIL-53(Al), NH₂-MIL-53(Al), and NHOCOCF₃-MIL-53(Al) was Al₂O₃.
 366 It should be mentioned that in this research MOFs are used as fillers for the modification
 367 of membranes operating below 100°C. Therefore, it can be considered that MOFs are stable
 368 under these conditions.



369
 370 Figure 7. Thermogravimetric analysis (A and B) of MIL-53(Al), NH₂-MIL-53(Al),
 371 and NHOCOCF₃-MIL-53(Al).
 372

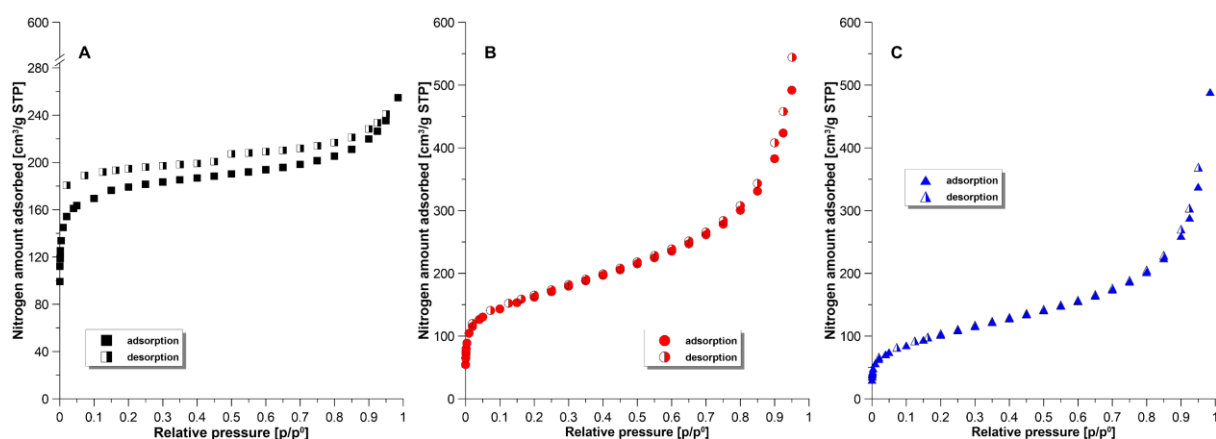
373 Specific surface area (S_{BET}), pore size, and pore volume (V_{pores}) of MIL-53(Al),
 374 NH₂-MIL-53(Al), and NHOCOCF₃-MIL-53(Al) were determined by measuring
 375 the N₂ adsorption isotherms at 73 K. Results are gathered in Figure 8 and Table 1.
 376 The adsorption isotherms of MIL-53(Al) and NH₂-MIL-53(Al) can be classified as Type I
 377 and Type IV, respectively [42] (Figure 8A and B) which is in good accordance with literature
 378 data [43-45].

379

380 Table 1. Comparison of S_{BET} , pore volume and pore diameter of MIL-53(Al), NH₂-MIL-53(Al),
 381 and NHOCOCF₃-MIL-53(Al).

Particles	S_{BET}	V_{pores}	V_{micro} (t-plot)	pore diameter
	[m ² g ⁻¹]	[cm ³ g ⁻¹]	[cm ³ g ⁻¹]	[Å]
MIL-53(Al)	584.70	0.28	0.25	9.21
NH ₂ -MIL-53(Al)	325.69	0.15	0.11	8.77
NHOCOCF ₃ -MIL-53(Al)	105.76	0.09	0.06	7.31

382



383

384 Figure 8. N₂ adsorption isotherm of A – MIL-53(Al), B – NH₂-MIL-53(Al),
 385 and C – NHOCOCF₃-MIL-53(Al).

386

387

388 The highest value of specific surface area (S_{BET}) was noticed for the MIL-53(Al), while
 389 the lowest one was for modified NHOCOCF₃-MIL-53(Al). MIL-53(Al) demonstrated
 390 a comparable value of S_{BET} with values reported in the literature [46].
 391 In the case of NH₂-MIL-53(Al), a lower value of S_{BET} was detected compared with the literature.
 392 The lower specific surface of NH₂-MIL-53(Al) could be related to the presence of the residual
 393 amounts of solvents (DMF and water) detected on TGA analysis (Figure 7).
 394 However, it should be mentioned that the solvent used for the synthesis of NH₂-MIL-53(Al)
 395 significantly affected the S_{BET} value and V_{pores} [34]. Cheng et al. [34] observed that when water
 396 ratio in DMF/water mixed solvents increased from 3.3% to 75%, S_{BET} decreased from 1882 m²
 397 g⁻¹ to 1088 m² g⁻¹ with a simultaneous increase of V_{pores} from 1.03 cm³ g⁻¹ to 1.30 cm³ g⁻¹.

397

398

399

400

401

402

403

404

405

406

407

408

409

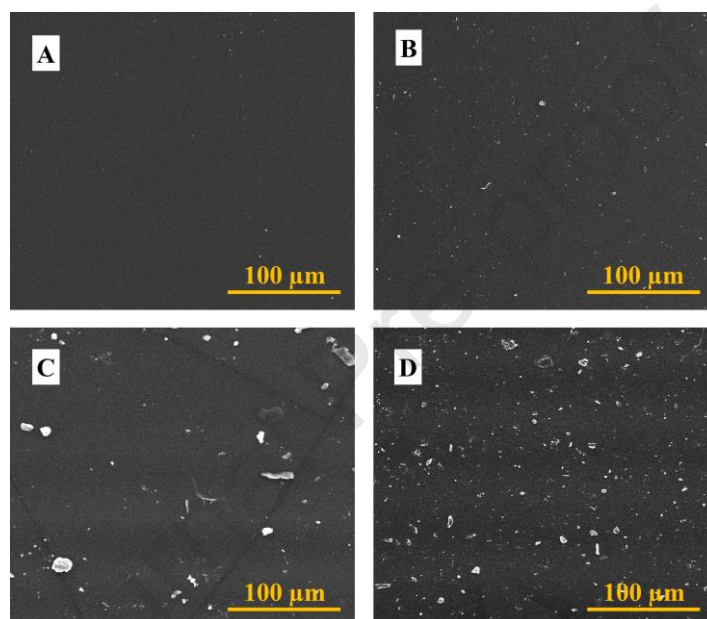
410

Moreover, it was also observed that modification of NH₂-MIL-53(Al) by trifluoroacetic
 anhydride caused degradation of a specific surface and pore size to 105.76 m² g⁻¹ and 7.31 Å,
 respectively. After modification, trifluoroacetic groups partially filled the pores of MOF
 particles. Moreover, the pore distribution of NH₂-MIL-53(Al) and NHOCOCF₃-MIL-53(Al)
 revealed that the modified NH₂-MIL-53(Al) had lower pore volume and micropore volume
 compared with the pristine NH₂-MIL-53(Al). A similar reduction of S_{BET} , pore size and pore
 volume was also reported in other post-synthetic modifications of NH₂-MIL-53(Al) [45-48].

411 3.2 Membrane characterization

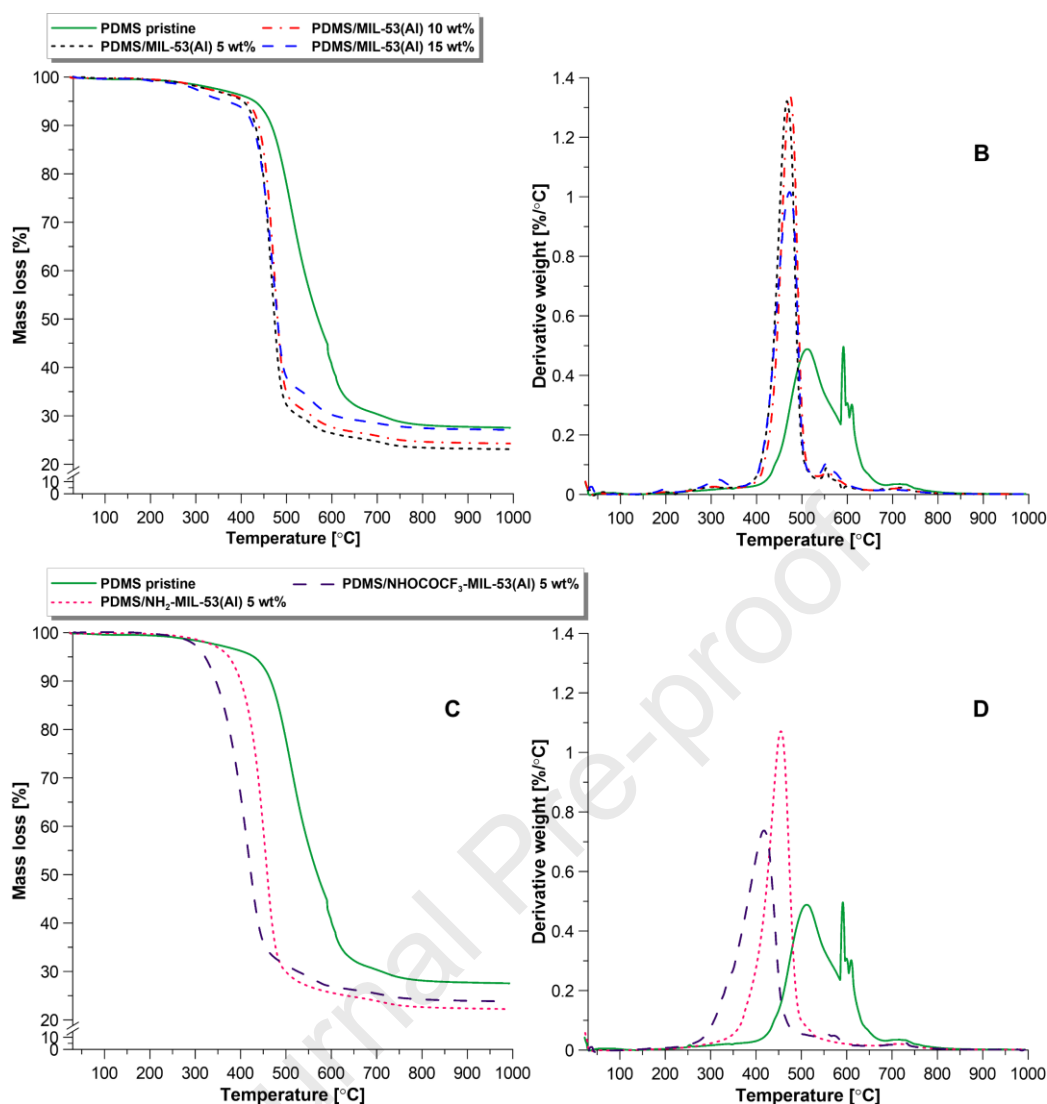
412 SEM analysis of the surface of pristine and heterogeneous membranes is shown
 413 in Figure 9. As it can be seen, SEM analysis proved the formation of dense membranes without
 414 visible porous structure (Figure 9A-D).

415 Moreover, in the case of PDMS membranes with 5 wt% MIL-53(Al)
 416 and NHOCOCF₃-MIL-53(Al) micrographs suggest good incorporation of MOF particles
 417 without agglomeration (Figure 9B and D). Agglomeration of particles was only detected
 418 for the PDMS membrane modified by 5 wt% of NH₂-MIL-53(Al) (Figure 9C).



419
 420 Figure 9. SEM micrographs of the surface of pristine PDMS (A), PDMS/MIL-53(Al) 5 wt% (B),
 421 PDMS/NH₂-MIL-53(Al) 5 wt% (C), and PDMS/NHOCOCF₃-MIL-53(Al) 5 wt% (D) membranes.

422
 423 Thermal properties of pristine PDMS and heterogeneous PDMS based membranes
 424 containing MIL-53(Al), NH₂-MIL-53(Al), and NHOCOCF₃-MIL-53(Al) were investigated
 425 using thermogravimetric analysis (Figure 10A-D). In the case of pristine PDMS membrane,
 426 it was observed that degradation of this membrane occurred as a one-step process.
 427 Cyclic hexamethylcyclotrisiloxane is a product of the degradation of poly(dimethylsiloxane)
 428 polymer [49] and PDMS based membranes are thermally stable up to 400°C (Figure 10A-D).
 429 As it can be seen from Figure 10, the degradation of heterogeneous PDMS based membranes
 430 containing MIL-53(Al), NH₂-MIL-53(Al), and NHOCOCF₃-MIL-53(Al) occurs through
 431 multiple stages. Moreover, it was also noticed that the incorporation of MOF particles slightly
 432 decreased the thermal stability of MMMs compared with a pristine PDMS.
 433 In the case of PDMS/NH₂-MIL-53(Al) 5 wt% and PDMS/NHOCOCF₃-MIL-53(Al) 5 wt%
 434 membranes are thermally stable up to 300°C and 250°C, respectively.

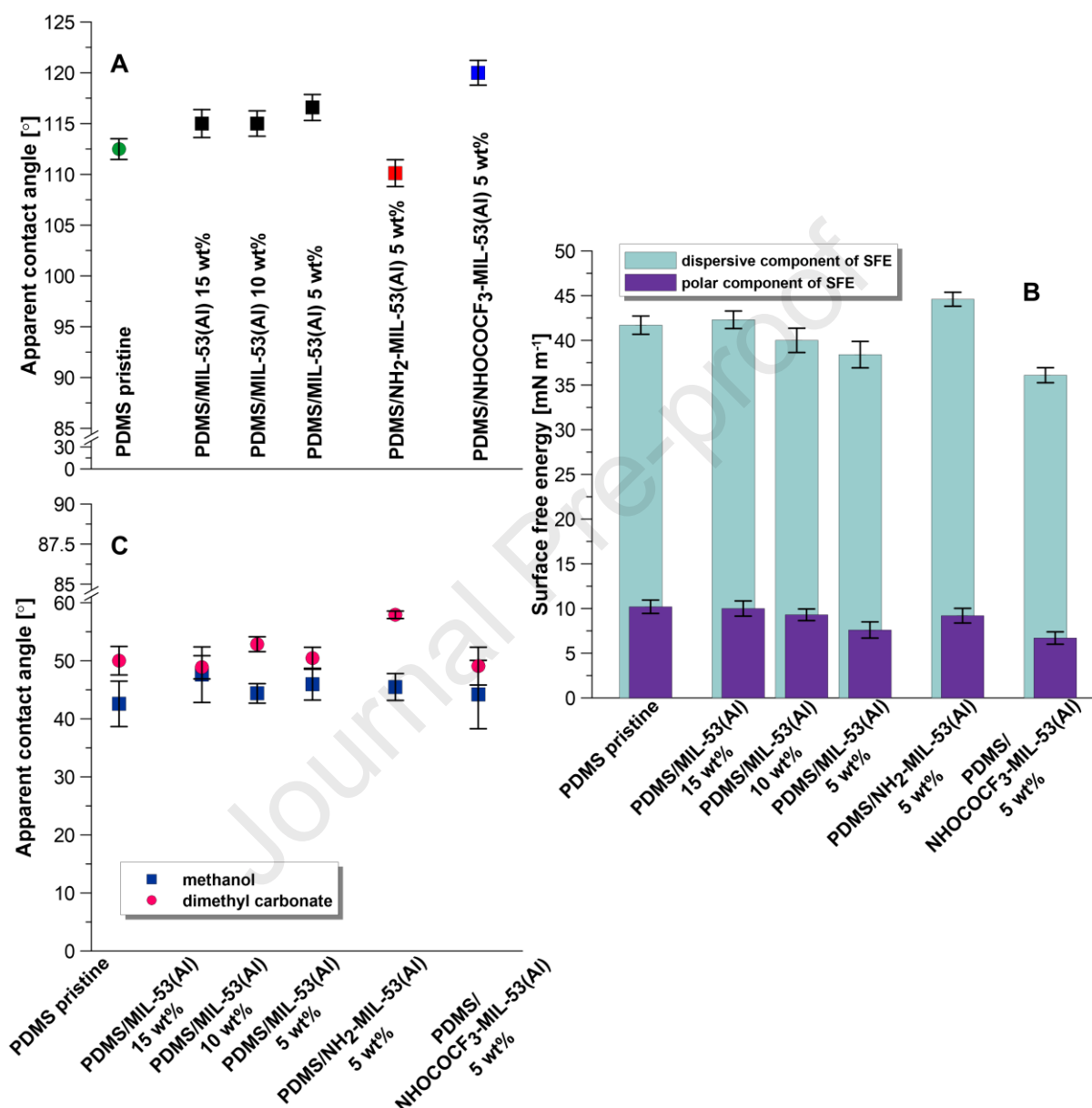


435
 436 Figure 10. TGA (A, C) and DTG (B, D) curves of pristine and heterogeneous PDMS-based membranes.
 437

438 Measurements of the contact angle for water and diiodomethane were performed
 439 to investigate the influence of the incorporation of MIL-53(Al), NH₂-MIL-53(Al),
 440 and NHOCOCF₃-MIL-53(Al) particles on membrane surface hydrophobicity.
 441 In the case of the modified membrane by the various amounts of MIL-53(Al), the alterations
 442 in wettability of the membrane surfaces are noticeable. The highest increase in contact angle
 443 from 113° for pristine PDMS membranes to 117° was found for the PDMS/MIL-53(Al) 5 wt%
 444 membranes (Figure 11A).

445 In the case of PDMS based membrane modified by 5 wt% of NH₂-MIL-53(Al), after
 446 incorporation of NH₂-MIL-53(Al), the contact angle of water decreased slightly from 113°
 447 to 110° (Figure 11A). The lower contact angle of water for PDMS/NH₂-MIL-53(Al) is related
 448 to the hydrophilic character of the NH₂-MIL-53(Al). NH₂-MIL-53(Al) contains hydrophilic
 449 amino NH₂ groups. Additionally, the PDMS membrane modified by 5 wt% of NH₂-MIL-53(Al)

450 is characterized by the highest R_A parameter (Figure S1 and Table S1). A similar trend was
 451 observed by Al-Shaeli et al. [50]. It was reported that the modification of the polyethersulfone
 452 (PES) ultrafiltration membrane by 5 wt% of UiO-66-NH₂ caused the reduction of the water
 453 contact angle from 80° to 44° [50].



454
 455 Figure 11. The apparent contact angle of water (A), calculated surface free energy (B) of pristine and
 456 heterogeneous PDMS-based membranes and apparent contact angle of methanol and dimethyl
 457 carbonate.

458
 459 Analysing the obtained results, it can be noticed that the PDMS membrane
 460 which contains hydrophobic NHOCOCF₃-MIL-53(Al) particles demonstrated a higher water
 461 contact angle (120°) compared with the pristine one (113°) (Figure 11A). It can be concluded
 462 that the incorporation of NHOCOCF₃-MIL-53(Al) increased the hydrophobic character

463 of the PDMS membrane. Han et al. [51] modified ZIF-90 with (3-aminopropyl) triethoxysilane
464 (APTES) using Schiff's base reaction. Subsequently, APTES-ZIF-90 particles
465 were used as a filler for the preparation of heterogeneous PDMS based membranes.
466 Analysing the values of the contact angle for water it was shown that the incorporation
467 of 5 wt% of APTES-ZIF-90 caused an increase in water contact angle from ca. 112° to 120°
468 [51].

469 The value of the contact angle for water and diiodomethane
470 was also used for the calculation of the surface free energy (SFE) by Owen's-Wendt's method
471 [52] (Figure 11B). According to Owen's-Wendt's theory, surface free energy (SFE)
472 is expressed by polar and dispersive components [52]. Taking into account of results
473 of the calculation, it was observed that the incorporation of 5 wt% of MIL-53(Al)
474 and NHOCOCF_3 -MIL-53(Al) leads to a decrease in the polar part of surface free energy.
475 As it can be seen from Figure 11B, PDMS/ NHOCOCF_3 -MIL-53(Al) 5 wt% membrane
476 demonstrated a 34% (6.7 mN m^{-1}) lower value of polar part of SFE compared with a pristine
477 PDMS one (10.0 mN m^{-1}) (Figure 11B). This confirms, that after modification
478 by 5 wt% of NHOCOCF_3 -MIL-53(Al), the hydrophobic character of the PDMS membrane
479 increased.

480 The contact angle of methanol and dimethyl carbonate for pristine and modified
481 membranes was also measured (Figure 11C). Both pristine and modified membranes showed
482 similar values of contact angle ($45.0 \pm 1.6^\circ$). In the case of contact angle of DMC,
483 only PDMS/ NH_2 -MIL-53(Al) demonstrated a much higher contact angle ($57.9 \pm 0.6^\circ$)
484 compared with the contact angle of methanol while rest membranes exhibited only a slightly
485 higher contact angle ($50.3 \pm 0.9^\circ$). The relatively low contact angle of methanol and dimethyl
486 carbonate for both pristine and modified PDMS-based membranes is related to the low surface
487 tension of PDMS (20.4 mN/m [53]). It means that PDMS is characterized by good wettability.
488 It should be also mentioned that the surface tension of MeOH and DMC is equal to 22.7 mN/m
489 [54] and 29.4 mN/m [55], respectively. Therefore, both methanol and dimethyl carbonate
490 can partially wet the surface of PDMS-based membranes. The slightly higher contact angle
491 of dimethyl carbonate could be related to the properties of the DMC. Dimethyl carbonate
492 is a nonpolar aprotic solvent while methanol is polar [56].

493
494
495
496

497 3.3 Hansen's Solubility Parameters

498 According to the solution-diffusion theory, transport and separation in pervaporation
 499 occurs in three subsequent stages: sorption, diffusion, and desorption [57]. Hansen's Solubility
 500 Parameters (HSP), especially the distance parameter (Δ , Eq. (5)) can be used for the estimation
 501 and prediction of relations between separated mixture/pure solvents and membrane [58] during
 502 the sorption step. According to the definition of the distance parameter, the lower the distance
 503 parameter is, the stronger interactions between solvent/mixture and membrane occur [58].

$$504 \Delta = \sqrt{(\delta_{d,S1} - \delta_{d,S2})^2 + (\delta_{p,S1} - \delta_{p,S2})^2 + (\delta_{h,S1} - \delta_{h,S2})^2} \quad (5)$$

505 where $\delta_{d,S1}$, $\delta_{d,S2}$ are dispersion interactions, $\delta_{p,S1}$, $\delta_{p,S2}$ are polar interactions, and $\delta_{h,S1}$, $\delta_{h,S2}$
 506 are hydrogen bonding interactions.

507 However, it should be emphasized that Eq. (5) can be used for pristine membranes
 508 and pure solvents. The situation became more complex when modified membranes
 509 were used for the separation of a mixture of solvents. The incorporation of various fillers into
 510 a polymer matrix changed the interaction between the membrane and separated mixtures.
 511 Therefore, before the calculation of distance parameters between MMMs and a mixture
 512 of solvents, modified Hansen's Solubility Parameters (δ_m) should be determined
 513 for both MMMs and a mixture of solvents. In the next step, using the modified HSP, distance
 514 parameters between MMMs and a mixture of solvents can be calculated. There are several
 515 approaches which can be applied for the determination of the modified HSP (Eq. (6)), however,
 516 Bagley's approach is the most suitable for the polymer membranes.

$$517 \delta_m = [\delta_d, \delta_p, \delta_h] = [(a \cdot \delta_{d1} + b \cdot \delta_{d2}), (a \cdot \delta_{p1} + b \cdot \delta_{p2}), (a \cdot \delta_{h1} + b \cdot \delta_{h2})]/(a + b) \quad (6)$$

518 where: δ_{d1} , δ_{p1} , δ_{h1} – dispersive, polar and hydrogen bonding interactions for the first component
 519 and δ_{d2} , δ_{p2} , δ_{h2} – dispersive, polar and hydrogen bonding interactions for the second
 520 component, a and b – mass fraction (wt.%) of the first and the second component, respectively.

521 In the case of polymeric membranes modified by MOF particles, the interaction between
 522 MOF particles and pure solvents/mixture of solvents depended not only on the dispersive,
 523 hydrogen, and polar interaction but also on the pore size of MOFs and kinetic dimensions of
 524 guest molecules [59]. There is a limiting research which estimated the parameter for MOF
 525 particles [12, 59, 60]. All of this research used the procedure proposed by Hansen [61].
 526 Nevertheless, the application of HSP to evaluate host–guest interactions involving MOFs is in
 527 the spotlight [59].

528 Hansen postulated that polymer-ligand interactions dominated the MOF-polymer
529 interaction and that the ligand's solubility parameters are equivalent to the solubility parameters
530 of the supplied MOF [61]. MOF particles are composed of metal ions and organic ligands. MIL-
531 53(Al), NH₂-MIL-53(Al), and NHOCOF₃-MIL-53(Al) are consisted of the same metal ion
532 (Al³⁺) but various ligands (BDC – MIL-53(Al), NH₂-BDC – NH₂-MIL-53(Al), and NHOCOF₃
533 – NHOCOF₃-MIL-53(Al)). The value of HSP parameters of NHOCOF₃-MIL-53(Al) was
534 calculated based on the van Krevelen group contribution method [62] (Table 2). The definition
535 of the SP does not cover the determination of solubility of a solid substance, *e.g.*, MOF. The
536 phase transition from the solid crystal to the liquid state prior to mixing as well as entropy
537 effects on solubility is not considered. The solubility parameters rather predict the enthalpic
538 contribution to the mixing energy by using the cohesion energy as measure of intermolecular
539 attraction in a respective liquid. Thereby, it relies on the chemical rule of similarity when it
540 comes to interaction between different species. In solid dosage forms, *e.g.*, polymer films, the
541 filler, *i.e.*, MOF is not interacting with the polymeric matrix. This case of solid dispersions is
542 described as solid amorphous suspensions. Regarding the application to solid dispersions, the
543 solubility parameter estimates the extent of interaction between filler and polymer on a
544 molecular scale which is an important condition for solubility. It does not provide direct
545 information on the solid state after mixing both compounds. This is why in some case, the HSP
546 need to be supported by group contribution parameters, *e.g.*, van Krevelen/Hoftyzer [63],
547 Breitskreutz [64], and Stefanis/Panayiotou [65].

548 Based on Hansen's approach it can be assumed that HSP for MIL-53(Al), NH₂-MIL-
549 53(Al), and NHOCOF₃-MIL-53(Al) are equal to HSP of BDC, NH₂-BDC, and NHOCOF₃,
550 respectively.

551

552

553

554 Table 2. Hansen's Solubility Parameters for polymer, solvents, and ligands.

Solvent, ligand or polymer	Hansen's Solubility Parameters [MPa ^{0.5}]			Ref.
	δ_d	δ_p	δ_h	
MeOH	15.1	12.3	22.3	[58]
DMC	15.5	8.6	9.7	[66]
BDC	20.0	7.2	12.8	[59]
NH ₂ -BDC	20.8	8.6	16.4	[59]
NHOCOCF ₃	18.4	9.7	17.5	-
PDMS	15.9	0.0	4.1	[36]
PDMS/MIL-53(Al) 5wt%	16.1	0.4	4.5	-
PDMS/MIL-53(Al) 10wt%	16.3	0.7	5.0	-
PDMS/MIL-53(Al) 15wt%	16.5	1.1	5.4	-
PDMS/NH ₂ -MIL-53(Al) 5wt%	16.2	0.4	4.7	-
PDMS/NHOCOCF ₃ -MIL-53(Al) 5wt%	16.2	0.9	5.2	-

555
556 Table 3. Calculated distance parameters (Δ) between PDMS based membranes and pure solvents (MeOH
557 and DMC).

Membranes	MeOH	DMC
	Δ [MPa ^{0.5}]	
PMDS	22.0	10.3
PDMS/MIL-53(Al) 5 wt%	21.4	9.7
PMDS/MIL-53(Al) 10 wt%	20.9	9.2
PDMS/MIL-53(Al) 15 wt%	20.6	8.7
PDMS/NH ₂ -MIL-53(Al) 5 wt%	21.2	9.6
PDMS/NHOCOCF ₃ -MIL-53(Al) 5 wt%	20.7	9.0

558
559 Table 4. Calculated distance parameters (Δ) between separated mixture (MeOH/DMC) and PDMS based
560 membranes.

Membranes	Δ [MPa ^{0.5}]				
	DMC/MeOH				
	20/80	30/70	50/50	70/30	80/20
PDMS	19.5	18.3	15.8	13.5	10.2
PDMS/MIL-53(Al) 5 wt%	18.9	17.7	15.3	13.0	9.7
PMDS/MIL-53(Al) 10 wt%	18.4	17.2	14.7	12.4	9.3
PDMS/MIL-53(Al) 15 wt%	17.8	16.6	14.2	11.9	8.8
PDMS/NH ₂ -MIL-53(Al) 5 wt%	18.8	17.5	15.1	12.8	9.6
PDMS/NHOCOCF ₃ -MIL-53(Al) 5 wt%	18.2	16.9	14.5	12.2	11.1

561 Calculated values of distance parameters for pure solvents (MeOH, DMC) and a mixture
562 of MeOH/DMC are gathered in Table 3 and 4. Analysing the distance parameter between
563 membranes and pure solvents (methanol and DMC), it can be concluded that the DMC should

564 be more selective toward PDMS membranes during the sorption step.
565 Moreover, it was also noticed that after the incorporation of MOF particles, the value of the
566 distance parameter decreased. Incorporation of MIL-53(Al), NH₂-MIL-53(Al)
567 and NHOCOCF₃-MIL-53(Al) into the PDMS matrix may improve the efficiency
568 of the heterogeneous membrane compared to a pristine one during the sorption step.
569 The distance parameter between solvents (MeOH, DMC) and PDMS membranes
570 (pristine and modified) decreased with an increasing amount of MIL-53(Al) in the polymer
571 matrix. The smallest value of Δ was found for the PDMS/MIL-53(Al) 15 wt% in contact
572 with DMC. In the case of the PDMS membranes modified by 5 wt% of fillers, it was observed
573 that the smallest value of the distance parameters was found for the PDMS/NHOCOCF₃-MIL-
574 53(Al) 5 wt% (Table 3 and 4). In light of this, it can be supposed that PDMS/NHOCOCF₃-
575 MIL-53(Al) 5 wt% should be more selective than PDMS/MIL-53(Al) 5 wt% and PDMS/NH₂-
576 MIL-53(Al) 5 wt% during the sorption stage.

577 Taking into consideration separated mixtures of dimethyl carbonate/methanol,
578 it was noticed that interaction between membranes (both pristine and heterogeneous)
579 and separated liquid mixtures increased with increasing content of dimethyl carbonate
580 in the mixture (Table 4). Similarly, to the interaction between membranes and pure solvents,
581 the distance parameter (Δ) decreased after the incorporation of MOFs. In the case of the mixture
582 containing 80 wt% of DMC, PDMS/NHOCOCF₃-MIL-53(Al) 5 wt% membrane showed
583 slightly higher Δ compared with pristine PDMS membranes. The smallest Δ parameter
584 was found for PDMS/MIL-53(Al) 15 wt% during the contact with 20/80 MeOH/DMC mixture
585 which is coherent with the abovementioned results.

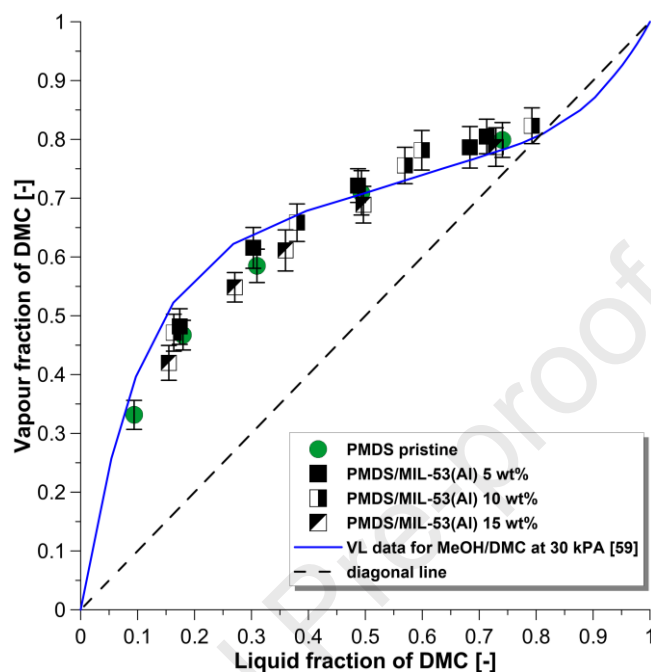
586

587 **3.4 Effectiveness of dimethyl carbonate/methanol separation using pervaporation**

588 The performance of a modified PDMS-based membrane in the pervaporative removal
589 of dimethyl carbonate from a dimethyl carbonate/methanol mixture was investigated at 40°C
590 and using the thickness normalized flux (Eqs. 1 and 2), the separation factor (Eq. 3),
591 and the thickness normalized Pervaporation Separation Index (Eq. 4). The thickness of tested
592 membranes was in the range of 228-395 μ m.

593 In the first stage of pervaporation experiments, PDMS-based membranes with various
594 amounts of MIL-53(Al) were tested to find the optimal content of particles in the PDMS matrix.
595 McCabe-Thiele diagrams present in Figure 12 revealed that both pristine and modified
596 membranes selectively transported dimethyl carbonate from separated mixtures.

597 It was observed that the vapour fraction of dimethyl carbonate in permeate increased with
 598 increasing the liquid fraction of DMC in the feed solution. Based on the data presented
 599 in Table 4, it was found that the affinity between the membranes and the separated mixture
 600 increased with the increasing content of DMC.



601
 602 Figure 12. McCabe-Thiele separation diagrams for PDMS, PDMS/MIL-53(Al) 5 wt%, PDMS/MIL-
 603 53(Al) 10 wt%, and PDMS/MIL-53(Al) 15 wt% membranes in contact with DMC/MeOH mixtures.
 604 Vapour-liquid (VL) equilibrium of MeOH and DMC data was taken from the work of Cho et al.[67].
 605

606 Figure 12 also presents the vapour-liquid for methanol and dimethyl carbonate. DMC
 607 and MeOH possess boiling points equal to 90.3 °C [68] and 64.7 °C [69], respectively.
 608 Based on this information it can be assumed that simple distillation
 609 can be used for the separation of DMC/MeOH. However, dimethyl carbonate and methanol
 610 create the azeotrope, therefore, simple distillation cannot be applied. The solution
 611 could be pressure-swing distillation, azeotropic distillation, and extractive distillation.
 612 Application of extractive and azeotropic distillation necessitates the incorporation of a mass-
 613 separating agent [70]. Extractive distillation is a process which uses the fluctuation of the
 614 azeotrope point with pressure [71]. Generally, all of these processes are very energy-intensive.
 615 The VL equilibrium demonstrated that the methanol/dimethyl carbonate mixture creates the
 616 azeotrope at 80 wt% of methanol, therefore distillation can not be applied to separate the
 617 mixture containing mixtures containing 80 wt% and more percent of methanol. At the same
 618 time, when the pervaporation was applied for the separation of this mixture, ca. 80 wt% of
 619 DMC. Based on these results, it can be concluded that the best option for the separation of the

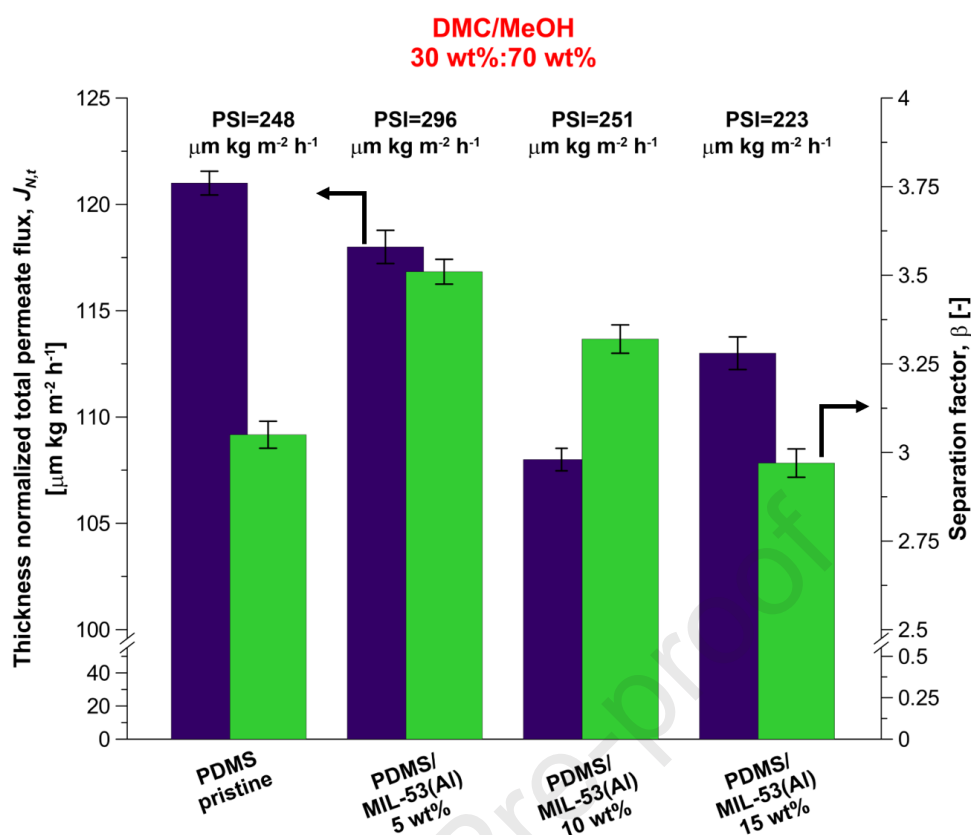
620 DMC/MeOH mixture could be a hybrid process containing distillation and pervaporation.
621 During the distillation, DMC/MeOH is separated to obtain azeotrope, then azeotrope is
622 separated by pervaporation. Such a solution combines the advantages of distillation (large
623 capacity) and pervaporation (high selectivity). Research performed by Norkobilov et al. [72]
624 showed that the application of a hybrid process (distillation followed by pervaporation) for
625 ethyl *tert*-butyl ether production can save 52% and 49% in heating and cooling utilities,
626 respectively [72].

627 Figure 13 demonstrates the comparison of the separation factors and thickness-
628 normalized total fluxes of pristine and heterogeneous PDMS-based membranes obtained during
629 the separation of the DMC/MeOH mixture containing 30 wt% of dimethyl carbonate.

630 It was noticed that in the case of PDMS membranes modified by 5 and 10 wt% of MIL-
631 53(Al), the separation factor (transport properties) increased while the thickness normalized
632 total flux (transport properties) slightly decreased after modification. PDMS/MIL-53(Al)
633 membrane demonstrated 1.13 higher value of separation factor ($\beta=3.5$) compared to the pristine
634 PDMS membrane ($\beta=3.1$) (Figure 13). Despite the lower transport properties of PDMS/MIL-
635 53(Al) 5 wt% and PDMS/MIL-53(Al) 10 wt% membranes compared with pristine PDMS,
636 these membranes revealed a higher value of PSI_N (Figure 13).

637 Thickness normalized Pervaporation Separation Index (PSI_N) is a valuable parameter
638 used for the assessment of various membranes applied in pervaporation. A comparison
639 of PSI_N values shows that the highest value of this parameter was found for the PDMS
640 membrane modified by 5 wt% of MIL-53(Al). The incorporation of 5 wt% of MIL-53(Al)
641 caused an increase in PSI_N from $248 \mu\text{m kg m}^{-2} \text{h}^{-1}$ to $296 \mu\text{m kg m}^{-2} \text{h}^{-1}$. The PDMS/MIL-
642 53(Al) 15 wt% membrane, membrane showed transport and separation properties lower than
643 the pristine PDMS one. It should be mentioned that the maximum filler content in the PDMS
644 polymer matrix was equal to 15 wt%. Above this amount, interactions between the filler and
645 the platinum catalyst stopped the crosslinking process and a stable membrane could be not
646 formed.

647 Based on the obtained results it can be concluded that 5 wt% of MIL-53(Al)
648 is an optimum amount of particles incorporated into the PDMS matrix. Therefore, in the next
649 part of this research, PDMS membranes were modified with 5 wt% of NH_2 -MIL-53(Al) and
650 NHOCOCF_3 -MIL-53(Al).



651

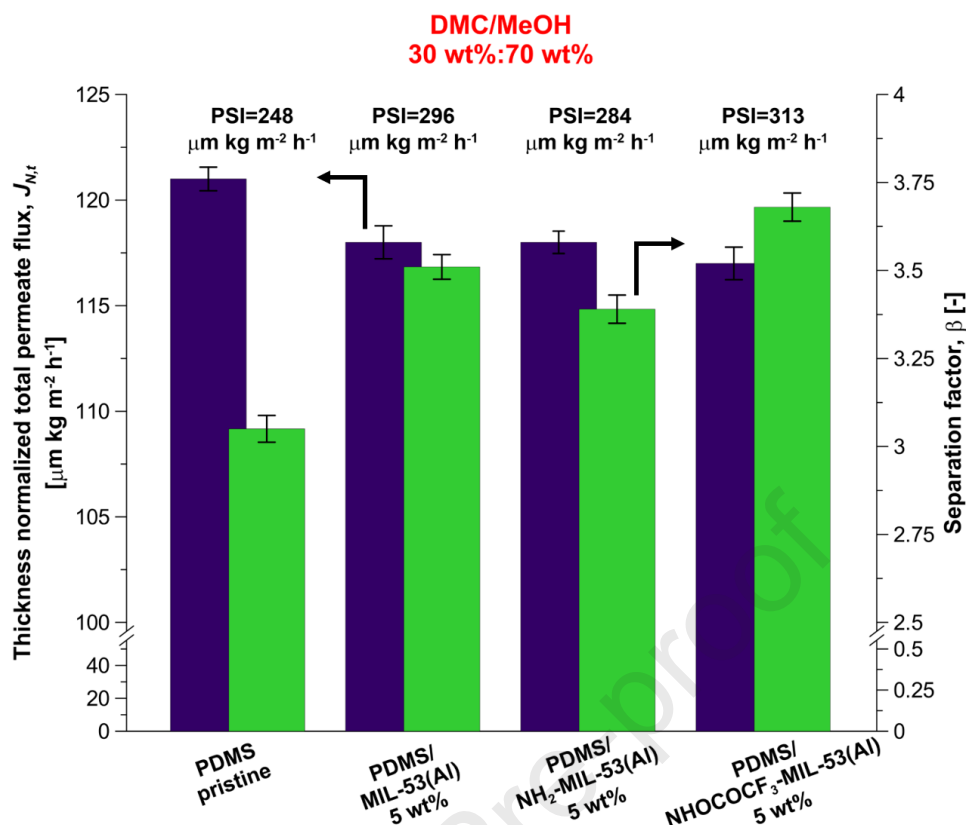
652 Figure 13. Comparison of the efficiency of pristine and heterogeneous PDMS-based membranes
 653 modified by 5, 10, and 15 wt% of MIL-53(Al). Feed mixture: DMC (30 wt%) – MeOH (70 wt%).

654

655 Results of the pervaporative separation of DMC/methanol using pristine PDMS
 656 and PDMS with 5 wt% of MIL-53(Al), NH₂-MIL-53(Al), and NHOCOCF₃-MIL-53(Al)
 657 membranes are presented in Figure 14.

658 Similarly to the PDMS/MIL-53(Al) membrane, the incorporation of 5 wt% of NH₂-
 659 MIL-53(Al) and NHOCOCF₃-MIL-53 influenced the separation properties of heterogeneous
 660 membranes. It was noticed that after modification, heterogeneous membranes possessed higher
 661 separation properties compared with pristine PDMS. MIL-53(Al), NH₂-MIL-53(Al), and
 662 NHOCOCF₃-MIL-53(Al) possessed different properties. Therefore, the incorporation of MIL-
 663 53(Al), NH₂-MIL-53(Al), and NHOCOCF₃-MIL-53(Al) into the PDMS matrix showed
 664 different impacts on the transport and separation properties of PDMS membranes. The highest
 665 value of the separation factor (β) was noticed for the membrane modified by NHOCOCF₃-MIL-
 666 53(Al). After the addition of hydrophobic NHOCOCF₃-MIL-53(Al) value of β increased from
 667 3.1 to 3.7 (Figure 14).

668



669

670 Figure 14. Comparison of the efficiency of pristine PDMS, PDMS/MIL-53(AI) 5 wt%, PDMS/NH₂-
 671 MIL-53(AI) 5 wt%, and PDMS/NHOCOCF₃-MIL-53(AI) membranes obtained during the separation of
 672 the DMC/MeOH mixture containing 30 wt% of DMC.

673

674 Based on the established results it can be concluded that the incorporation
 675 of hydrophobized MIL-53(AI) is the best choice to improve the efficiency of recovery of DMC
 676 from a dimethyl carbonate/methanol mixture. The experimental data are consistent with HSP
 677 calculations (Table 4). The distance parameter (Δ) for the pristine membrane was equal
 678 to 18.3 MPa^{0.5} and was reduced to 16.9 MPa^{0.5} after the introduction of the hydrophobic
 679 NHOCOCF₃-MIL-53(AI). Taking into account the transport properties, it was observed
 680 that after the modification total permeate flux slightly decreased. The incorporation of 5 wt%
 681 of NHOCOF₃-MIL-53(AI) into PDMS reduced the total flux from 121 $\mu\text{m kg m}^{-2} \text{h}^{-1}$
 682 (for pristine PDMS) to 117 $\mu\text{m kg m}^{-2} \text{h}^{-1}$. However, it should be mentioned that both pristine
 683 PDMS and PDMS/NHOCOCF₃-MIL-53(AI) 5 wt% membranes demonstrated similar DMC
 684 permeate flux equal to 71 $\mu\text{m kg m}^{-2} \text{h}^{-1}$ and 73 $\mu\text{m kg m}^{-2} \text{h}^{-1}$, respectively. While the MeOH
 685 flux was reduced, it was observed that the MeOH flux decreased from 50 $\mu\text{m kg m}^{-2} \text{h}^{-1}$
 686 for the pristine PDMS membrane to 44 $\mu\text{m kg m}^{-2} \text{h}^{-1}$ for the PDMS/NHOCOCF₃-MIL-53(AI)
 687 5 wt% one.

688 In the case of PDMS/NH₂-MIL-53(Al) 5 wt% membrane, the membrane demonstrated
689 the lowest transport and separation properties among the heterogeneous PDMS based
690 membranes. This is related to the least hydrophobic character of the PDMS/NH₂-MIL-53(Al)
691 membrane. According to the calculated value of SFE, this membrane is characterized
692 by the highest value of the polar part of SFE and it also demonstrated a lower value
693 of the contact angle of water compared to PDMS/MIL-53(Al) and PDMS/NHOCOCF₃-MIL-
694 53(Al) membranes (Figure 11A and B). The lower efficiency of the PDMS/NH₂-MIL-53(Al)
695 membrane could be also connected with the agglomeration of fillers detected by SEM analysis
696 (Figure 9C).

697 According to the solution-diffusion mechanism, separation in pervaporation is related
698 to the different affinities of the separated components to the membrane, while diffusion
699 of separated components depends on free volume in the polymer matrix and the molecular size
700 of the penetrant [57]. The incorporation of porous MIL-53(Al), NH₂-MIL-53(Al), and
701 NHOCOCF₃-MIL-53(Al) rearranged the conformation of polymer chains and the value of free
702 volume increased. Based on the nitrogen adsorption/desorption measurements, pore sizes of
703 MIL-53(Al), NH₂-MIL-53(Al), and NHOCOCF₃-MIL-53(Al) are higher than the kinetic
704 diameter of methanol (3.6 Å [14]) and dimethyl carbonate (between 4.7 and 6.3 Å [73]). Both
705 separated components can pass through the pores of used fillers. It is known that when the pore
706 size of the MOF particle is slightly larger than the kinetic diameter of separated components,
707 separation occurs by the difference in diffusion rates of components [74]. Methanol and
708 dimethyl carbonate possess different properties, methanol is polar, while dimethyl carbonate is
709 a nonpolar aprotic solvent [56]. In the case of hydrophobic NHOCOCF₃-MIL-53(Al), dimethyl
710 carbonate is more preferentially transported through the pores of this filler and interfacial
711 regions around the filler, while methanol is rejected. Therefore, PDMS/NHOCOCF₃-MIL-
712 53(Al) 5 wt% demonstrated the best efficiency in the separation of the dimethyl
713 carbonate/methanol mixture. Whereas, regarding the hydrophilic NH₂-MIL-53(Al), methanol
714 is transported to a greater extent through the pores of this filler and around the interfacial region
715 compared to the MIL-53(Al) and NHOCOCF₃-MIL-53(Al). Consequently, PDMS/NH₂-MIL-
716 53(Al) revealed the lowest efficiency in the removal of DMC from binary DMC/MeOH
717 mixture.

718

719 **3.5 Comparison with literature data**

720 Table 5 compares the efficiency of PDMS/MIL-53(Al) 5 wt% and PDMS/NHOCOCF₃-
 721 MIL-53(Al) 5 wt% membranes in the removal of DMC from the DMC/MeOH mixture with
 722 efficiencies of various hydrophobic membranes used for the separation of the same mixture.
 723 The comparison shows that PDMS/NHOCOCF₃-MIL-53(Al) 5 wt% demonstrated the
 724 comparable value of separation factor and slightly lower value of total flux. However, it should
 725 be emphasized that membranes used in this research were obtained by incorporating a lower
 726 amount of fillers (5 wt%) compared with the literature data (30 wt%). The lower amount of
 727 fillers added into the polymer matrix may reduce the agglomeration of fillers and also the
 728 overall cost of the preparation of Mixed Matrix Membranes.

729 Furthermore, the comparison revealed a typical trend observed in pervaporation,
 730 i.e., increasing the temperature of experiments causes an increase in the value of the total flux
 731 with a simultaneous decrease in the separation factor (Table 5).

732

733 Table 5. Comparison of the efficiency of various PDMS membranes in the removal of DMC
 734 from the azeotropic DMC/methanol mixture containing 30 wt% of DMC.

Membrane	T	DMC content	J_T	β	Refs.
	[°C]	[wt %]	[kg m ⁻² h ⁻¹]	[-]	
PDMS/PVDF	40	28	0.48	3.9	[10]
PDMS/DNS-2 15 wt%	40	30	0.71	3.9	[9]
RTV	50	30	ca. 1.8	3.7	[75]
PAN/RTV/nano SiO ₂ 30 wt%	50	30	ca. 3.8	4.4	[75]
PDMS/MCM-41 30 wt%	40	30	ca. 0.8	3.8	[16]
PDMS/MCM-41 30 wt%	60	30	ca. 2.5	2.2	[16]
PDMS	40	30	0.60	3.1	this work
PDMS/MIL-53(Al) 5 wt%	40	30	0.56	3.5	this work
PDMS/NHOCOCF ₃ -MIL-53(Al) 5 wt%	40	30	0.55	3.7	this work

735

3.6 Influence of traces of water in the feed solution on the separation efficiency of the DMC/MeOH mixture

The influence of water presence in organic solvents on the overall efficiency of organic-organic pervaporation was also investigated using the enrichment factor of water (Eq. (5)) as a metric. EF_{water} higher than unity indicates the preferential transport of water from feed to permeate side. It should be mentioned that water presence in the feed solution of investigated mixtures was in the range of 0.1 to 0.2 wt%.

The obtained values of the enrichment factor of water are gathered in Table 6. The comparison showed that all PDMS-based membranes demonstrated a value of EF_{water} higher than unity, which means that water was preferentially transported from the feed to the permeate side. It can be explained by the fact, that water possesses a much lower kinetic diameter compared with methanol and dimethyl carbonate. During pervaporation, membranes swelled in contact with MeOH and DMC, therefore, small water molecules could easily be transported through the membranes, regardless of their polar nature.

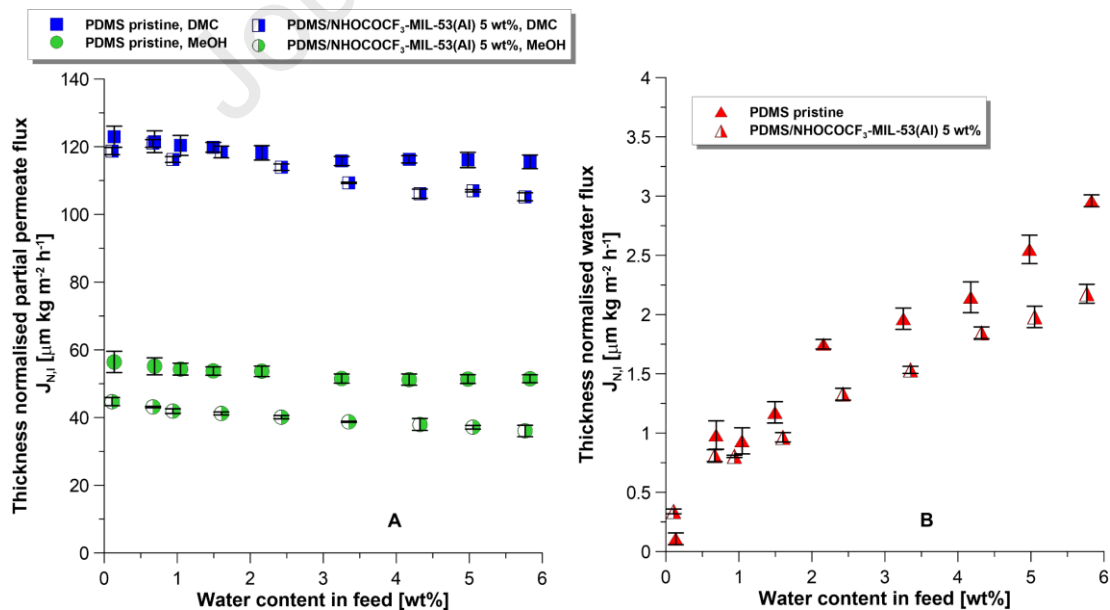
Taking into account the results with MMMs, it was noticed that the incorporation of particles decreased the transport of water across the membranes. The lowest value of the enrichment factor of water was found for the PDMS membrane modified by the hydrophobic $NHOCOCF_3$ -MIL-53(Al). The incorporation of 5 wt% of hydrophobic particles caused the reduction of EF_{water} by 54% compared to the pristine PDMS membrane. The reduction of water transport through the membranes during the organic-organic pervaporation is crucial for the further development of organic solvent separation by pervaporation. Indeed, the excessive presence of water in permeate might cause the occurrence of a two-phase system and lead to the corrosion of the piping system.

PDMS/ NH_2 -MIL-53(Al) 5 wt% and PDMS/MIL-53(Al) 15 wt% membranes demonstrated slightly higher values of EF_{water} compared with the pristine PDMS membrane. In the case of the PDMS membrane modified with 5 wt% of NH_2 -MIL-53(Al) higher EF_{water} could be connected with the hydrophilic character of NH_2 -MIL-53(Al) particles (Figure 11). Regarding the PDMS/MIL-53(Al) 15 wt% membrane higher water transport could be related to the agglomerates detected on the surface of the membrane (Figure S2).

766 Table 6. Comparison of the calculated value of enrichment factor of water (EF_{water}) for pristine
 767 and modified PDMS based membranes (mixture of DMC/MeOH 30:70).

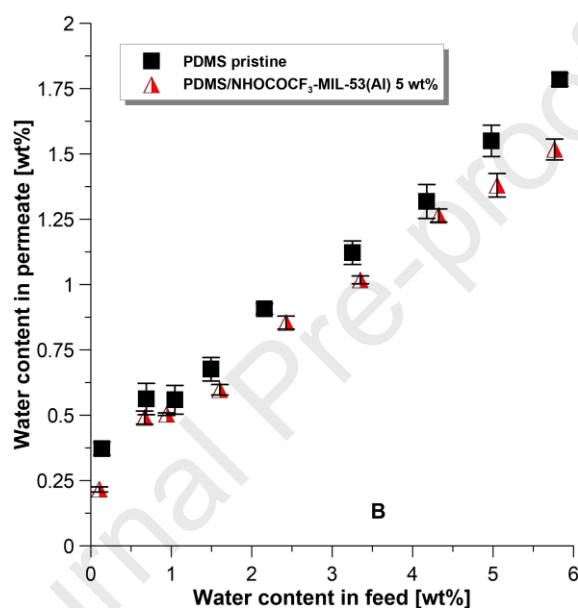
Membranes	EF_{water}
	[-]
PMDS	2.7
PDMS/MIL-53(Al) 5 wt%	1.8
PDMS/MIL-53(Al) 10 wt%	2.0
PDMS/MIL-53(Al) 15 wt%	2.8
PDMS/NH ₂ -MIL-53(Al) 5 wt%	2.9
PDMS/NHOCOCF ₃ -MIL-53(Al) 5 wt%	1.3

768 One of the most common methods used for the production of dimethyl carbonate is oxy-
 769 -carbonylation of methanol on a CuCl catalyst [76]. Usually, the reactor contains 50–70 wt%
 770 of methanol, 30–40 wt% of dimethyl carbonate and 2–5 wt% of water [77]. After synthesis, the
 771 obtained mixture consists of 51.9 wt% methanol, 42.8 wt% DMC and 5.3 wt% water [78].
 772 Therefore, in this research, the influence of increasing water content in DMC/MeOH on
 773 pervaporation efficiency was also investigated. In that case, pervaporation experiments were
 774 performed with a DMC/MeOH (equimass) mixture and increasing the content of water from
 775 0.1 to 6 wt%. Based on the obtained results (Figure 14 and Table 6), two membranes were
 776 selected for further investigation, i.e., pristine PDMS and PDMS/NHOCOCF₃-MIL-53(Al) 5
 777 wt%.



778 Figure 15. Comparison of thickness normalized partial fluxes of DMC and MeOH (A). Comparison of
 779 thickness normalized water flux (B).
 780
 781

782 The transport properties of the membranes are shown in Figure 15. It was observed
 783 that up to 3 wt% of water in a DMC/MeOH mixture, fluxes of dimethyl carbonate and methanol
 784 decreased (Figure 15A). A more significant change in the value of thickness normalized partial
 785 permeate fluxes, especially for DMC was noticed for the PDMS/NHOCOCF₃-MIL-53(Al)
 786 5 wt% membrane. Above 3 wt% of water in the feed mixture, the fluxes of methanol
 787 and dimethyl carbonate stabilized. In the case of water flux, it was observed that water flux
 788 increased with increasing content of water in the feed solution (Figure 15B) and a slightly
 789 higher water flux was noticed for the pristine PDMS membrane.



790
 791 Figure 16. Water content in permeate as a function of water content in the feed mixture
 792 (DMC/MeOH 50 wt%:50 wt%).

793
 794 Figure 16 presents the comparison of water content in permeate for pristine PDMS
 795 and PDMS/NHOCOCF₃-MIL-53(Al) 5 wt% membranes. Results indicated that water content
 796 in permeate increased with increasing content of water in feed. PDMS is characterized
 797 by a hydrophobic character, therefore the transport of water through the membrane should
 798 be suppressed. During the pervaporation with a DMC/MeOH mixture containing ca. 5.8 wt%
 799 of water in feed, in the permeate, only 1.8 wt% and 1.5 wt% were detected for the pristine
 800 PDMS and PDMS/NHOCOCF₃-MIL-53(Al) 5 wt% membranes, respectively.
 801 It can be concluded that the incorporation of hydrophobic particles is a good way to reduce
 802 the transport of water from feed to the permeate side.

803

804 Table 7. Comparison of experimental data for separation of DMC/MeOH mixture (50 wt%:50 wt%)
 805 with increased the content of water in the feed mixture for PDMS/NHOCOCF₃-MIL-53(Al) 5 wt%
 806 membrane.

Water content in feed [wt%]	MeOH content [wt%]		DMC content [wt%]	
	feed	permeate	feed	permeate
0.1	50.5	28.5	49.4	71.3
0.7	49.8	26.1	49.5	73.4
0.9	48.4	26.4	50.7	73.1
1.6	46.5	25.6	51.9	73.7
2.4	47.7	25.8	49.9	73.3
3.4	48.1	25.7	48.5	73.3
4.3	49.2	25.5	46.5	73.2
5.8	49.8	25.1	44.4	73.4

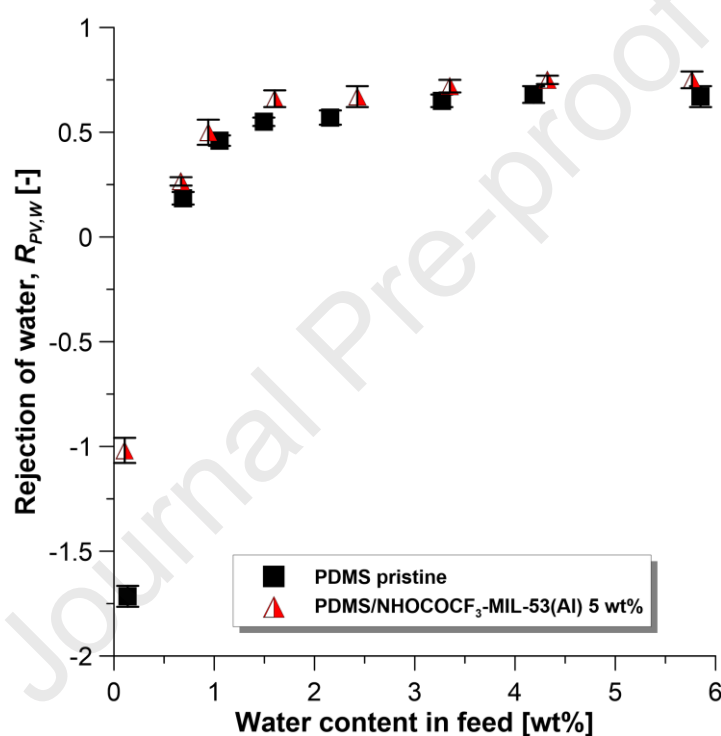
807
 808 A comparison of experimental data for PDMS/NHOCOCF₃-MIL-53(Al) 5 wt%
 809 membrane is presented in Table 7. It can be seen that when the water content in the feed
 810 increased, the content of MeOH in the permeate decreased. Whereas the content of DMC
 811 in permeate remained unchanged. These results may indicate that separated compounds
 812 were not transported independently and couplings between methanol and water transport occur
 813 (Table 7 and S2). The coupling effect is a very complex phenomenon and could be described
 814 by e.g. changes in solubility and activity of components in the polymer matrix [79].
 815 In this research, the coupling effect could be related to the similar properties of water
 816 and methanol. Both methanol and water are polar components in contrast
 817 to the nonpolar dimethyl carbonate. During pervaporation, methanol molecules interact
 818 with water molecules and the H-bondings between methanol and water molecules are created
 819 [80]. Therefore water together was with methanol transported through the membrane.
 820 A much stronger coupling effect was observed by Won et al. [76]. The authors tested
 821 the efficiency of the hydrophilic chitosan membrane in the separation of a ternary
 822 (DMC/MeOH/H₂O) mixture containing 1.1 wt% and 6.8 wt% of water. It was noticed
 823 that with increasing content of water (from 1.1 wt% to 6.8 wt%) the methanol content
 824 in permeate decreased from 86.3 wt% to 73.0 wt%. At the same time, the water content
 825 in permeate increased from 11.2 wt% to 24.2 wt%. Additionally, no influence of water presence
 826 in feed solution on DMC concentration in permeate was observed [76].

827 Parameter rejection of water $R_{PV,W}$ was used to evaluate and discuss the ability
 828 of rejection of water by pristine PDMS and PDMS/NHOCOCF₃-MIL-53(Al) 5 wt%
 829 membranes. The rejection of water was calculated based on Eq. (8) and the results
 830 of the calculation are presented in Figure 17.

$$831 \quad R_{PV,W} = \frac{F_W - P_W}{F_W} \quad (6)$$

832 The pristine PDMS membrane demonstrated smaller values of rejection
 833 of water compared with the PDMS/NHOCOCF₃-MIL-53(Al) 5 wt%. It can be concluded
 834 that the incorporation of a hydrophobic modifier slightly increases the efficiency
 835 in the rejection of water. However, it should be mentioned that the character of the used
 836 membrane (hydrophilic or hydrophobic) mainly influenced the transport of water from the feed
 837 to the permeate. An interesting observation was noticed for the experiments
 838 with DMC/methanol with traces amount of water (ca. 0.1 wt% of water).
 839 In the case of this mixture negative rejection of water was observed (-1.7 and -1.0 for pristine
 840 and modified PDMS membrane, respectively) (Figure 17). These results are directly related
 841 to the calculated EF_{water} (Table 6). This means, that despite the hydrophobic character
 842 of the PDMS membrane, water is selectively transported through the membrane.
 843 When the content of water in the feed increased from ca. 0.1 wt% to ca. 0.7 wt%,
 844 both membranes demonstrated a positive value of $R_{PV,W}$ coefficient. In the case of the feed
 845 mixture containing ca. 0.7 wt% of water, the water content in the permeate was 19% (for pristine
 846 PDMS) and 27% (for PDMS/NHOCOCF₃-MIL-53(Al) 5 wt%) lower in comparison with the
 847 content of water in the feed solution (Figure 17). As it was mentioned before during the sorption
 848 step, the membrane swelled, the relaxation of polymer chains took place and the free volume
 849 of polymer increased. Swelling of the membrane is especially high during the organic-organic
 850 pervaporation. At the very low content of water (traces amount), due to the swelling
 851 of the PDMS membranes, such a small amount of water together with methanol can easily pass
 852 through the membrane. When the water content in the feed solution increased (starting from ca.
 853 0.7 wt%, Figure 17) the affinity of both PDMS-based membranes towards the separated mixture
 854 decreased. It was noticed that Δ parameter between membranes and feed solution increased
 855 with increasing content of water in the feed solution (Tables S3-S5). Despite the swelling of
 856 the membrane, both pristine and modified PDMS membranes begin to reduce the transport of
 857 water molecules through the membranes. Negative rejection was also noticed by
 858 Darvishmanesh et al. [81]. The authors studied the efficiency of STARMEM™122 membrane
 859 in the rejection of Sudan II, Sudan Black, and Sudan 408. Analyzing the obtained results, it was
 860 observed that the STARMEM™122 membrane demonstrated negative rejection when the *n*-
 861 hexane was used as a solvent. In other cases (when methanol, ethanol, acetone, methyl ethyl
 862 ketone, and toluene were used as a solvent) positive values of rejection were observed. It should
 863 be mentioned that the molecular weight of the selected dye (Sudan II – 276.33 g mol⁻¹, Sudan

864 Black – $456.54 \text{ g mol}^{-1}$, and Sudan 408 – $464.60 \text{ g mol}^{-1}$) was above the MWCO of membrane
 865 (220 g mol^{-1}). It is suggested that the rejection value is influenced not only by the MWCO of
 866 the selected membrane but also by the interaction (calculated based on Hansen's Solubility of
 867 Parameters) between solvent and membrane and solute and membrane. In the case of
 868 experiments
 869 with *n*-hexane, a higher affinity between solute (dye) and membrane was noticed compared
 870 to an affinity between solvent (*n*-hexane) and membrane. Despite the higher MWCO
 871 of the STARMEM™122 membrane, Sudan II, Sudan Black, and Sudan 408 were selectively
 872 transported through the membrane.



873
 874 Figure 17. Comparison in the efficiency of rejection of water for pristine PDMS
 875 and PDMS/NHOCOCF₃-MIL-53(Al) 5 wt% membranes.
 876

877 Additionally, it was also observed that with increasing content of water in feed,
 878 the rejection coefficient increased and reached a stable value of ca. 0.67 and 0.76 for pristine
 879 PDMS and PDMS/NHOCOCF₃-MIL-53(Al) 5 wt% membranes, respectively.
 880

881 4. Conclusions

882 Hydrophobic NHOCOCF₃-MIL-53(Al) was successfully synthesized
 883 and for the first time, incorporated into a PDMS matrix for the separation of dimethyl carbonate
 884 from methanol. XRD analysis confirmed the crystal structure of MOF particles, additionally,

885 it was also confirmed that post-synthesis modification of NH₂-MIL-53(Al) did not influence
886 the crystal structure of NH₂-MIL-53(Al). The particle sizes measured with TEM and DLS
887 techniques were coherent, and an increase in the studied values proved the accomplished
888 modification. A comparison of the BET surface area of NH₂-MIL-53(Al) and NHOCOCF₃-
889 MIL-53(Al) revealed that after modification, the specific surface area decreased owing to the
890 attachment of trifluoroacetic anhydride. The Hansen Solubility Parameters were implemented
891 to understand the interactions between the membrane and solvents during the sorption as well
892 as how the modification of the membrane influenced these interactions. The implemented
893 functionalization process allows for an increase in the affinity between the membrane matrix
894 and dimethyl carbonate. The best affinity was found for the PDMS functionalized with
895 NHOCOCF₃-MIL-53(Al) 5 wt%. At an optimal filler loading (5 wt%), the NHOCOCF₃-MIL-
896 53(Al) increase the separation properties compared to the pristine PDMS membrane.
897 Improvement of the separation efficiency was related to the creation of a permeable region
898 selective toward DMC. PDMS/NHOCOCF₃-MIL-53(Al) 5 wt% membrane enhanced the
899 separation of DMC with 119% (from 3.1 to 3.7). A comparison with literature data related to
900 PDMS-based membranes showed that PDMS based membrane with only 5 wt% of
901 NHOCOCF₃-MIL-53(Al) 5 wt% demonstrated the comparable value of separation factor with
902 PDMS membranes containing a high amount of fillers (30 wt%). The undoubted advantage of
903 modification with a small amount of modifier is the reduction of the modifier agglomeration.
904 The influence of water presence in the feed solution was also investigated. The obtained results
905 indicated the presence of a coupling effect between methanol and water molecules. The
906 coupling effect could be explained by the swelling of the membranes and the creation of the H-
907 bondings between the water and methanol molecules. Interesting results were noticed for the
908 mixture containing traces amount of water (ca. 0.1 wt%). It was found that despite the
909 hydrophobic character of both pristine and modified PDMS membranes,
910 water was preferentially transported from the feed to the permeate side. Both membranes
911 demonstrated EF_{water} results higher than unity and negative value of $R_{PV,w}$. This phenomenon
912 could be related to the swelling of the membranes. A quite different phenomenon was observed
913 for the mixtures containing a higher amount of water in the feed solution, as it was found that
914 both membranes partially suppressed the transport of water molecules. The possible
915 explanation for this behaviour could be the decreasing the affinity between the membrane and
916 the separated mixture when increasing the water content.

917 **CRedit authorship contribution statement**

918 **Katarzyna Knozowska:** Conceptualization, Formal analysis, Funding acquisition,
919 Investigation, Methodology, Validation, Visualization, Writing – original draft.

920 **Tadeusz Muzioł:** Formal analysis, Writing - review & editing.

921 **Joanna Kujawa:** Formal analysis, Writing - review & editing.

922 **Anthony Szymczyk:** Writing - review & editing.

923 **Wojciech Kujawski:** Supervision, Writing - review & editing.

924

925 **References**

926 [1] H.S. Varyemez, D.B. Kaymak, Effect of operating pressure on design of extractive
927 distillation process separating DMC-MeOH azeotropic mixture, *Chem. Eng. Res. Des.*, 177
928 (2022) 108-116. <https://doi.org/10.1016/j.cherd.2021.10.029>.

929 [2] M.A. Pacheco, C.L. Marshall, Review of dimethyl carbonate (DMC) manufacture and its
930 characteristics as a fuel additive, *Energy Fuels*, 11 (1997) 2-29.
931 <https://doi.org/10.1021/ef9600974>.

932 [3] Y. Ono, Catalysis in the production and reactions of dimethyl carbonate, an environmentally
933 benign building block, *Appl. Catal., A*, 155 (1997) 133-166. [https://doi.org/10.1016/S0926-](https://doi.org/10.1016/S0926-860X(96)00402-4)
934 [860X\(96\)00402-4](https://doi.org/10.1016/S0926-860X(96)00402-4).

935 [4] Z. Zhang, H. Xu, Q. Zhang, A. Zhang, Y. Li, W. Li, Separation of methanol + dimethyl
936 carbonate azeotropic mixture using ionic liquids as entrainers, *Fluid Phase Equilib.*, 435 (2017)
937 98-103. <https://doi.org/10.1016/j.fluid.2016.11.026>.

938 [5] J.H. Chen, Q.L. Liu, A.M. Zhu, Q.G. Zhang, J. Fang, Pervaporation separation of
939 MeOH/DMC mixtures using STA/CS hybrid membranes, *J. Membr. Sci.*, 315 (2008) 74-81.
940 <https://doi.org/10.1016/j.memsci.2008.02.017>.

941 [6] H. Zhu, R. Li, G. Liu, Y. Pan, J. Li, Z. Wang, Y. Guo, G. Liu, W. Jin, Efficient separation
942 of methanol/dimethyl carbonate mixtures by UiO-66 MOF incorporated chitosan mixed-matrix
943 membrane, *J. Membr. Sci.*, 652 (2022) 120473. <https://doi.org/10.1016/j.memsci.2022.120473>.

944 [7] G. Wu, M. Jiang, T. Zhang, Z. Jia, Tunable Pervaporation Performance of Modified MIL-
945 53(Al)-NH₂/Poly(vinyl Alcohol) Mixed Matrix Membranes, *J. Membr. Sci.*, 507 (2016) 72-80.
946 <https://doi.org/10.1016/j.memsci.2016.01.048>.

947 [8] L. Wang, J. Li, Y. Lin, C. Chen, Separation of dimethyl carbonate/methanol mixtures by
948 pervaporation with poly(acrylic acid)/poly(vinyl alcohol) blend membranes, *J. Membr. Sci.*,
949 305 (2007) 238-246. <https://doi.org/10.1016/j.memsci.2007.08.008>.

- 950 [9] L. Wang, X. Han, J. Li, X. Zhan, J. Chen, Separation of azeotropic
951 dimethylcarbonate/methanol mixtures by pervaporation: Sorption and diffusion behaviors in
952 the pure and nano silica filled pdms membranes, *Sep. Purif. Technol.*, 46 (2011) 1396-1405.
953 <https://doi.org/10.1080/01496395.2011.571227>.
- 954 [10] H. Zhou, L. Lv, G. Liu, W. Jin, W. Xing, PDMS/PVDF composite pervaporation
955 membrane for the separation of dimethyl carbonate from a methanol solution, *J. Membr. Sci.*,
956 471 (2014) 47-55. <https://doi.org/10.1016/j.memsci.2014.07.068>.
- 957 [11] K. Knozowska, J. Kujawa, R. Lagzdins, A. Figoli, W. Kujawski, A New Type of
958 Composite Membrane PVA-NaY/PA-6 for Separation of Industrially Valuable Mixture
959 Ethanol/Ethyl Tert-Butyl Ether by Pervaporation, *Materials*, 13 (2020) 3676.
960 <https://doi.org/10.3390/ma13173676>.
- 961 [12] K. Knozowska, R. Thür, J. Kujawa, I. Kolesnyk, I.F.J. Vankelecom, W. Kujawski,
962 Fluorinated MOF-808 with various modulators to fabricate high-performance hybrid
963 membranes with enhanced hydrophobicity for organic-organic pervaporation, *Sep. Purif.*
964 *Technol.*, 264 (2021) 118315. <https://doi.org/10.1016/j.seppur.2021.118315>.
- 965 [13] T. Borjigin, F. Sun, J. Zhang, K. Cai, H. Ren, G. Zhu, A microporous metal-organic
966 framework with high stability for GC separation of alcohols from water, *Chem. Commun.*, 48
967 (2012) 7613-7615. <https://doi.org/10.1039/C2CC33023G>.
- 968 [14] Y. Tang, D. Dubbeldam, S. Tanase, Water-Ethanol and Methanol-Ethanol Separations
969 Using in Situ Confined Polymer Chains in a Metal-Organic Framework, *ACS applied materials*
970 *& interfaces*, 11 (2019) 41383-41393. <https://doi.org/10.1021/acsami.9b14367>.
- 971 [15] O. Vopička, K. Pilnáček, K. Friess, Separation of methanol-dimethyl carbonate vapour
972 mixtures with PDMS and PTMSP membranes, *Sep. Purif. Technol.*, 174 (2017) 1-11.
973 <https://doi.org/10.1016/j.seppur.2016.09.041>.
- 974 [16] L. Wang, X. Han, J. Li, D. Zheng, L. Qin, Modified MCM-41 silica spheres filled
975 polydimethylsiloxane membrane for dimethylcarbonate/methanol separation via pervaporation,
976 *J. Appl. Polym. Sci.*, 127 (2013) 4662-4671. <https://doi.org/10.1002/app.38046>.
- 977 [17] T.R.E. Simpson, B. Parbhoo, J.L. Keddie, The dependence of the rate of crosslinking in
978 poly(dimethyl siloxane) on the thickness of coatings, *Polymer*, 44 (2003) 4829-4838.
979 [https://doi.org/10.1016/S0032-3861\(03\)00496-8](https://doi.org/10.1016/S0032-3861(03)00496-8).
- 980 [18] G. Liu, W. Jin, Pervaporation membrane materials: Recent trends and perspectives, *J.*
981 *Membr. Sci.*, 636 (2021) 119557. <https://doi.org/10.1016/j.memsci.2021.119557>.
- 982 [19] R. Khan, W.-M. Liu, I.U. Haq, H.-G. Zhen, H. Mao, Z.-P. Zhao, Fabrication of highly
983 selective PEBA mixed matrix membranes by incorporating metal-organic framework MIL-53

- 984 (Al) for the pervaporation separation of pyridine-water mixture, *J. Membr. Sci.*, 686 (2023)
985 122014. <https://doi.org/10.1016/j.memsci.2023.122014>.
- 986 [20] H. Heydari, S. Salehian, S. Amiri, M. Soltanieh, S.A. Musavi, UV-cured polyvinyl alcohol-
987 MXene mixed matrix membranes for enhancing pervaporation performance in dehydration of
988 ethanol, *Polym. Test.*, 123 (2023) 108046.
989 <https://doi.org/10.1016/j.polymertesting.2023.108046>.
- 990 [21] X. Zhan, R. Ge, S. Yao, J. Lu, X. Sun, J. Li, Enhanced pervaporation performance of PEG
991 membranes with synergistic effect of cross-linked PEG and porous MOF-508a, *Sep. Purif.*
992 *Technol.*, 304 (2023) 122347. <https://doi.org/10.1016/j.seppur.2022.122347>.
- 993 [22] J. Winarta, A. Meshram, F. Zhu, R. Li, H. Jafar, K. Parmar, J. Liu, B. Mu, Metal-organic
994 framework-based mixed-matrix membranes for gas separation: An overview, *J. Polym. Sci.*, 58
995 (2020) 2518-2546. <https://doi.org/10.1002/pol.20200122>.
- 996 [23] M. Amirilargani, R.B. Merlet, P. Hedayati, A. Nijmeijer, L. Winnubst, L.C.P.M. de Smet,
997 E.J.R. Sudhölter, MIL-53(Al) and NH₂-MIL-53(Al) modified α -alumina membranes for
998 efficient adsorption of dyes from organic solvents, *Chem. Commun.*, 55 (2019) 4119-4122.
999 <https://doi.org/10.1039/C9CC01624D>.
- 1000 [24] T. Loiseau, C. Serre, C. Huguenard, G. Fink, F. Taulelle, M. Henry, T. Bataille, G. Férey,
1001 A Rationale for the Large Breathing of the Porous Aluminum Terephthalate (MIL-53) Upon
1002 Hydration, *Eur. J. Chem.*, 10 (2004) 1373-1382. <https://doi.org/10.1002/chem.200305413>.
- 1003 [25] P. Kumar, K. Vellingiri, K.-H. Kim, R.J.C. Brown, M.J. Manos, Modern progress in metal-
1004 organic frameworks and their composites for diverse applications, *Microporous Mesoporous*
1005 *Mater.*, 253 (2017) 251-265. <https://doi.org/10.1016/j.micromeso.2017.07.003>.
- 1006 [26] X. Qian, B. Yadian, R. Wu, Y. Long, K. Zhou, B. Zhu, Y. Huang, Structure stability of
1007 metal-organic framework MIL-53 (Al) in aqueous solutions, *Int. J. Hydrogen Energy*, 38 (2013)
1008 16710-16715. <https://doi.org/10.1016/j.ijhydene.2013.07.054>.
- 1009 [27] J. García-Ben, J. López-Beceiro, R. Artiaga, J. Salgado-Beceiro, I. Delgado-Ferreiro, Y.V.
1010 Kolen'ko, S. Castro-García, M.A. Señarís-Rodríguez, M. Sánchez-Andújar, J.M. Bermúdez-
1011 García, Discovery of Colossal Breathing-Caloric Effect under Low Applied Pressure in the
1012 Hybrid Organic-Inorganic MIL-53(Al) Material, *Chem. Mater.*, 34 (2022) 3323-3332.
1013 <https://doi.org/10.1021/acs.chemmater.2c00137>.
- 1014 [28] J.L. de Miranda, T.P. de Abreu, J.M.B. Neto, D. de Pontes Souza, I. Coelho, F. Stavale,
1015 S.d.S.A. Oliveira, L.C. de Moura, A case study for an eco-design of aluminum terephthalate
1016 metal-organic framework- MIL-53(Al) for CO₂ and methane adsorption, *Sustainable Mater.*
1017 *Technol.*, 37 (2023) e00689. <https://doi.org/10.1016/j.susmat.2023.e00689>.

- 1018 [29] L.-H. Schilling, H. Reinsch, N. Stock, Synthesis, Structure, and Selected Properties of
1019 Aluminum-, Gallium-, and Indium-Based Metal–Organic Frameworks, in: S. Kaskel (Ed.) The
1020 Chemistry of Metal–Organic Frameworks, Wiley-VCH, Weinheim, 2016, pp. 105-135,
1021 <https://doi.org/10.1002/9783527693078.ch5>.
- 1022 [30] W.P. Mounfield, K.S. Walton, Effect of synthesis solvent on the breathing behavior of
1023 MIL-53(Al), *J. Colloid Interface Sci.*, 447 (2015) 33-39.
1024 <https://doi.org/10.1016/j.jcis.2015.01.027>.
- 1025 [31] J. Liu, F. Zhang, X. Zou, G. Yu, N. Zhao, S. Fan, G. Zhu, Environmentally friendly
1026 synthesis of highly hydrophobic and stable MIL-53 MOF nanomaterials, *Chem. Commun.*, 49
1027 (2013) 7430-7432. <https://doi.org/10.1039/C3CC42287A>.
- 1028 [32] J. Canivet, A. Fateeva, Y. Guo, B. Coasne, D. Farrusseng, Water adsorption in MOFs:
1029 fundamentals and applications, *Chem. Soc. Rev.*, 43 (2014) 5594-5617.
1030 <https://doi.org/10.1039/C4CS00078A>.
- 1031 [33] J.G. Nguyen, S.M. Cohen, Moisture-Resistant and Superhydrophobic Metal–Organic
1032 Frameworks Obtained via Postsynthetic Modification, *J. Am. Chem. Soc.*, 132 (2010) 4560-
1033 4561. <https://doi.org/10.1021/ja100900c>.
- 1034 [34] X. Cheng, A. Zhang, K. Hou, M. Liu, Y. Wang, C. Song, G. Zhang, X. Guo, Size- and
1035 morphology-controlled NH₂-MIL-53(Al) prepared in DMF–water mixed solvents, *Dalton*
1036 *Trans.*, 42 (2013) 13698-13705. <https://doi.org/10.1039/C3DT51322J>.
- 1037 [35] J. Kujawa, M. Głodek, I. Koter, B. Ośmiałowski, K. Knozowska, S. Al-Gharabli, L.F.
1038 Dumée, W. Kujawski, Molecular Decoration of Ceramic Supports for Highly Effective Enzyme
1039 Immobilization—Material Approach, *Materials*, 14 (2021) 201.
1040 <https://doi.org/10.3390/ma14010201>.
- 1041 [36] A. Kujawska, K. Knozowska, J. Kujawa, W. Kujawski, Influence of downstream pressure
1042 on pervaporation properties of PDMS and POMS based membranes, *Sep. Purif. Technol.*, 159
1043 (2016) 68-80. <https://doi.org/10.1016/j.seppur.2015.12.057>.
- 1044 [37] R.W. Baker, J.G. Wijmans, Y. Huang, Permeability, permeance and selectivity: A
1045 preferred way of reporting pervaporation performance data, *J. Membr. Sci.*, 348 (2010) 346-
1046 352. <https://doi.org/10.1016/j.memsci.2009.11.022>.
- 1047 [38] A. Kujawska, K. Knozowska, J. Kujawa, G. Li, W. Kujawski, Fabrication of PDMS based
1048 membranes with improved separation efficiency in hydrophobic pervaporation, *Sep. Purif.*
1049 *Technol.*, 234 (2020) 116092. <https://doi.org/10.1016/j.seppur.2019.116092>.

- 1050 [39] R. W. Baker, J.G. Wijmans, Y. Huang, Permeability, permeance and selectivity: A
1051 preferred way of reporting pervaporation performance data, *J. Membr. Sci.*, 348 (2010) 346-
1052 352. <https://doi.org/10.1016/j.memsci.2009.11.022>.
- 1053 [40] S. Couck, E. Gobechiya, C.E.A. Kirschhock, P. Serra-Crespo, J. Juan-Alcañiz, A. Martinez
1054 Joaristi, E. Stavitski, J. Gascon, F. Kapteijn, G.V. Baron, J.F.M. Denayer, Adsorption and
1055 Separation of Light Gases on an Amino-Functionalized Metal–Organic Framework: An
1056 Adsorption and In Situ XRD Study, *ChemSusChem*, 5 (2012) 740-750.
1057 <https://doi.org/10.1002/cssc.201100378>.
- 1058 [41] N. Reimer, B. Gil, B. Marszalek, N. Stock, Thermal post-synthetic modification of Al-
1059 MIL-53–COOH: systematic investigation of the decarboxylation and condensation reaction,
1060 *Crystengcomm*, 14 (2012) 4119-4125. <https://doi.org/10.1039/C2CE06649A>.
- 1061 [42] K.S.W. Sing, D.H. Everett, R.A.W. Haul, L. Moscou, R.A. Pierotti, J. Rouquérol, T.
1062 Siemieniewska, Reporting Physisorption Data for Gas/Solid Systems With Special Reference
1063 to the Determination of Surface Area and Porosity, Zürich, 1985,
1064 <https://www.degruyter.com/view/IUPAC/iupac.57.0007,2020-02-05t15:41:47.119+01:00>
- 1065 [43] T. Homburg, C. Hartwig, H. Reinsch, M. Wark, N. Stock, Structure property relationships
1066 affecting the proton conductivity in imidazole loaded Al-MOFs, *Dalton Trans.*, 45 (2016)
1067 15041-15047. <https://doi.org/10.1039/C6DT03048C>.
- 1068 [44] G. Zhang, R. Wo, Z. Sun, L. Xiao, G. Liu, G. Hao, H. Guo, W. Jiang, Amido-
1069 Functionalized Magnetic Metal–Organic Frameworks Adsorbent for the Removal of Bisphenol
1070 A and Tetracycline, *Front. Chem.*, 9 (2021). <https://doi.org/10.3389/fchem.2021.707559>.
- 1071 [45] L. Liu, X. Tai, X. Zhou, L. Liu, Synthesis, post-modification and catalytic properties of
1072 metal-organic framework NH₂-MIL-53(Al), *Chem. Res. Chin. Univ.*, 33 (2017) 231-238.
1073 <https://doi.org/10.1007/s40242-017-6420-7>.
- 1074 [46] S. Kavak, H.M. Polat, H. Kulak, S. Keskin, A. Uzun, MIL-53(Al) as a Versatile Platform
1075 for Ionic-Liquid/MOF Composites to Enhance CO₂ Selectivity over CH₄ and N₂, *Chem.: Asian*
1076 *J.*, 14 (2019) 3655-3667. <https://doi.org/10.1002/asia.201900634>.
- 1077 [47] B. Han, X. Xiao, L. Zhang, Y. Li, D. Wang, W. Ni, l-Cysteine functionalized NH₂-MIL-
1078 53(Al) for Pb²⁺ and Ni²⁺ removal from aqueous solution, *JCIS Open*, 1 (2021) 100003.
1079 <https://doi.org/10.1016/j.jciso.2021.100003>.
- 1080 [48] B. Veisi, B. Lorestani, S. Sobhan Ardakani, M. Cheraghi, L. Tayebi, Post synthetic
1081 modification of magnetite @MIL-53(Fe)-NH₂ core-shell nanocomposite for magnetic solid
1082 phase extraction of ultra-trace Pd(II) ions from real samples, *Int. J. Environ. Anal. Chem.*,
1083 (2022) 1-18. <https://doi.org/10.1080/03067319.2022.2032007>.

- 1084 [49] G. Camino, S.M. Lomakin, M. Lazzari, Polydimethylsiloxane thermal degradation Part 1.
1085 Kinetic aspects, *Polymers*, 42 (2001) 2395-2402. <https://doi.org/10.1016/S0032->
1086 3861(00)00652-2.
- 1087 [50] M. Al-Shaeli, S.J.D. Smith, S. Jiang, H. Wang, K. Zhang, B.P. Ladewig, Long-term stable
1088 metal organic framework (MOF) based mixed matrix membranes for ultrafiltration, *J. Membr.*
1089 *Sci.*, 635 (2021) 119339. <https://doi.org/10.1016/j.memsci.2021.119339>.
- 1090 [51] Z. Han, Y. Zhao, H. Jiang, A. Sheng, H. Li, H. Jia, Z. Yun, Z. Wei, H. Wang, (3-
1091 Aminopropyl) Triethoxysilane-Modified ZIF-90 Nanoparticle/Polydimethylsiloxane Mixed
1092 Matrix Membranes for Ethanol Recovery via Pervaporation, *ACS Appl. Nano Mater.*, 5 (2022)
1093 183-194. <https://doi.org/10.1021/acsanm.1c02523>.
- 1094 [52] D.K. Owens, R.C. Wendt, Estimation of the surface free energy of polymers, *J. Appl.*
1095 *Polym. Sci.*, 13 (1969) 1741-1747. <https://doi.org/10.1002/app.1969.070130815>.
- 1096 [53] S.V. Gohil, S. Suhail, J. Rose, T. Vella, L.S. Nair, Chapter 8 - Polymers and Composites
1097 for Orthopedic Applications, in: S. Bose, A. Bandyopadhyay (Eds.) *Materials for Bone*
1098 *Disorders*, Academic Press, 2017, pp. 349-403, [https://doi.org/10.1016/B978-0-12-802792-](https://doi.org/10.1016/B978-0-12-802792-9.00008-2)
1099 9.00008-2.
- 1100 [54] M. Součková, J. Klomfar, J. Pátek, Measurement and Correlation of the Surface
1101 Tension–Temperature Relation for Methanol, *J. Chem. Eng. Data*, 53 (2008) 2233-2236.
1102 <https://doi.org/10.1021/je8003468>.
- 1103 [55] F. Wang, J. Wu, Z. Liu, Surface tension of dimethyl carbonate (C₃H₆O₃), *Fluid Phase*
1104 *Equilib.*, 220 (2004) 123-126. <https://doi.org/10.1016/j.fluid.2004.03.002>.
- 1105 [56] S.-H. Pyo, J.H. Park, T.-S. Chang, R. Hatti-Kaul, Dimethyl carbonate as a green chemical,
1106 *Curr. Opin. Green Sustainable Chem.*, 5 (2017) 61-66.
1107 <https://doi.org/10.1016/j.cogsc.2017.03.012>.
- 1108 [57] J.G. Wijmans, R.W. Baker, The solution-diffusion model: a review, *J. Membr. Sci.*, 107
1109 (1995) 1-21. [http://dx.doi.org/10.1016/0376-7388\(95\)00102-I](http://dx.doi.org/10.1016/0376-7388(95)00102-I).
- 1110 [58] C.M. Hansen, *Hansen Solubility Parameters. A User's Book*, second ed., CRC Press,
1111 London, New York, 2007, <https://doi.org/10.1201/9781420006834>.
- 1112 [59] L. Paseta, G. Potier, S. Abbott, J. Coronas, Using Hansen solubility parameters to study
1113 the encapsulation of caffeine in MOFs, *Org. Biomol. Chem.*, 13 (2015) 1724-1731.
1114 <https://doi.org/10.1039/C4OB01898B>.
- 1115 [60] D. Elangovan, U. Nidoni, I.E. Yuzay, S.E.M. Selke, R. Auras, Poly(l-lactic acid) Metal
1116 Organic Framework Composites. Mass Transport Properties, *Ind. Eng. Chem. Res.*, 50 (2011)
1117 11136-11142. <https://doi.org/10.1021/ie201378u>.

- 1118 [61] C.M. Hansen, Polymer science applied to biological problems: Prediction of cytotoxic drug
1119 interactions with DNA, *Eur. Polym. J.*, 44 (2008) 2741-2748.
1120 <https://doi.org/10.1016/j.eurpolymj.2008.07.005>.
- 1121 [62] S. Just, F. Sievert, M. Thommes, J. Breitzkreutz, Improved group contribution parameter
1122 set for the application of solubility parameters to melt extrusion, *Eur. J. Pharm. Biopharm.*, 85
1123 (2013) 1191-1199. <https://doi.org/10.1016/j.ejpb.2013.04.006>.
- 1124 [63] D.W. Van Krevelen, Properties of polymers: their correlation with chemical structure: their
1125 numerical estimation and prediction from additive group contributions, fourth ed., Elsevier,
1126 Amsterdam, 2009,
- 1127 [64] J. Breitzkreutz, Prediction of intestinal drug absorption properties by three- dimensional
1128 solubility parameters, *Pharm. Res.*, 15 (1998) 1370-1375.
1129 <https://doi.org/10.1023/A:1011941319327>.
- 1130 [65] E. Stefanis, C. Panayiotou, A new expanded solubility parameter approach, *Int. J. Pharm.*,
1131 426 (2012) 29-43. <https://doi.org/10.1016/j.ijpharm.2012.01.001>.
- 1132 [66] S. Abbott, HSP Basics, [https://www.stevenabbott.co.uk/practical-solubility/hsp-](https://www.stevenabbott.co.uk/practical-solubility/hsp-basics.php)
1133 [basics.php](https://www.stevenabbott.co.uk/practical-solubility/hsp-basics.php), 2022, accessed 10 June 2022
- 1134 [67] J. Cho, Y.M. Kim, J. Noh, D.S. Kim, J. Cho, Experimental Study of Vapor-Liquid
1135 Equilibrium and Optimization of Pressure-Swing Distillation for Methanol-Dimethyl
1136 Carbonate Binary System, *Asian J. Chem.*, 26 (2014) 6769-6779.
1137 <https://doi.org/10.14233/ajchem.2014.16741>.
- 1138 [68] K. Takeuchi, 5.16 - Polycarbonates, in: K. Matyjaszewski, M. Möller (Eds.) *Polymer*
1139 *Science: A Comprehensive Reference*, Elsevier, Amsterdam, 2012, pp. 363-376,
1140 <https://doi.org/10.1016/B978-0-444-53349-4.00148-5>.
- 1141 [69] G.A. Olah, Beyond Oil and Gas: The Methanol Economy, *Angew. Chem., Int. Ed.*, 44
1142 (2005) 2636-2639. <https://doi.org/10.1002/anie.200462121>.
- 1143 [70] C.-C. Hu, S.-H. Cheng, Development of alternative methanol/dimethyl carbonate
1144 separation systems by extractive distillation — A holistic approach, *Chem. Eng. Res. Des.*, 127
1145 (2017) 189-214. <https://doi.org/10.1016/j.cherd.2017.09.016>.
- 1146 [71] W.L. Luyben, Importance of pressure-selection in pressure-swing distillation, *Comput.*
1147 *Chem. Eng.*, 149 (2021) 107279. <https://doi.org/10.1016/j.compchemeng.2021.107279>.
- 1148 [72] A. Norkobilov, D. Gorri, I. Ortiz, Comparative study of conventional, reactive-distillation
1149 and pervaporation integrated hybrid process for ethyl tert-butyl ether production, *Chem. Eng.*
1150 *Process.*, 122 (2017) 434-446. <https://doi.org/10.1016/j.cep.2017.07.003>.

- 1151 [73] T. Tsuru, A. Sasaki, M. Kanazashi, T. Yoshioka, Pervaporation of methanol/dimethyl
1152 carbonate using SiO₂ membranes with nano-tuned pore sizes and surface chemistry, *Aiche J.*,
1153 57 (2011) 2079-2089. <https://doi.org/10.1002/aic.12436>.
- 1154 [74] X. Li, Y. Liu, J. Wang, J. Gascon, J. Li, B. Van der Bruggen, Metal–organic frameworks
1155 based membranes for liquid separation, *Chem. Soc. Rev.*, 46 (2017) 7124-7144.
1156 <https://doi.org/10.1039/C7CS00575J>.
- 1157 [75] Z. Liu, W. Lin, Q. Li, Q. Rong, H. Zu, M. Sang, Separation of dimethyl carbonate/methanol
1158 azeotropic mixture by pervaporation with dealcoholized room temperature-vulcanized silicone
1159 rubber/nanosilica hybrid active layer, *Sep. Purif. Technol.*, 248 (2020) 116926.
1160 <https://doi.org/10.1016/j.seppur.2020.116926>.
- 1161 [76] W. Won, X. Feng, D. Lawless, Pervaporation with chitosan membranes: separation of
1162 dimethyl carbonate/methanol/water mixtures, *J. Membr. Sci.*, 209 (2002) 493-508.
1163 [https://doi.org/10.1016/S0376-7388\(02\)00367-8](https://doi.org/10.1016/S0376-7388(02)00367-8).
- 1164 [77] C. Guo, F. Wang, J. Xing, P. Cui, Thermodynamic and economic comparison of extractive
1165 distillation sequences for separating methanol/dimethyl carbonate/water azeotropic mixtures,
1166 *Sep. Purif. Technol.*, 282 (2022) 120150. <https://doi.org/10.1016/j.seppur.2021.120150>.
- 1167 [78] J.D. Medrano-García, J. Javaloyes-Antón, D. Vázquez, R. Ruiz-Femenia, J.A. Caballero,
1168 Alternative carbon dioxide utilization in dimethyl carbonate synthesis and comparison with
1169 current technologies, *J. CO₂ Util.*, 45 (2021) 101436.
1170 <https://doi.org/10.1016/j.jcou.2021.101436>.
- 1171 [79] W. Li, P. Luis, Understanding coupling effects in pervaporation of multi-component
1172 mixtures, *Sep. Purif. Technol.*, 197 (2018) 95-106.
1173 <https://doi.org/10.1016/j.seppur.2017.12.041>.
- 1174 [80] N. Zhang, Z. Shen, C. Chen, G. He, C. Hao, Effect of hydrogen bonding on self-diffusion
1175 in methanol/water liquid mixtures: A molecular dynamics simulation study, *J. Mol. Liq.*, 203
1176 (2015) 90-97. <https://doi.org/10.1016/j.molliq.2014.12.047>.
- 1177 [81] S. Darvishmanesh, J. Degrève, B. Van der Bruggen, Mechanisms of solute rejection in
1178 solvent resistant nanofiltration: the effect of solvent on solute rejection, *Phys. Chem. Chem.*
1179 *Phys.*, 12 (2010) 13333-13342. <https://doi.org/10.1039/C0CP00230E>.

1180

Highlights

- A simple and successful synthesis of hydrophobic hydrophobized analogue of MIL-53(AI)
- Novel PDMS MMM membrane for enhanced removal of DMC from DMC/MeOH mixture
- Implementation of HSP approach for discussion of pervaporation results
- Detailed evaluation of water content in DMC/MeOH feed mixture on PV efficiency

Journal Pre-proof

Declaration of interests

The authors declare that they have no known competing financial interests or personal relationships that could have appeared to influence the work reported in this paper.

The authors declare the following financial interests/personal relationships which may be considered as potential competing interests:

Journal Pre-proof